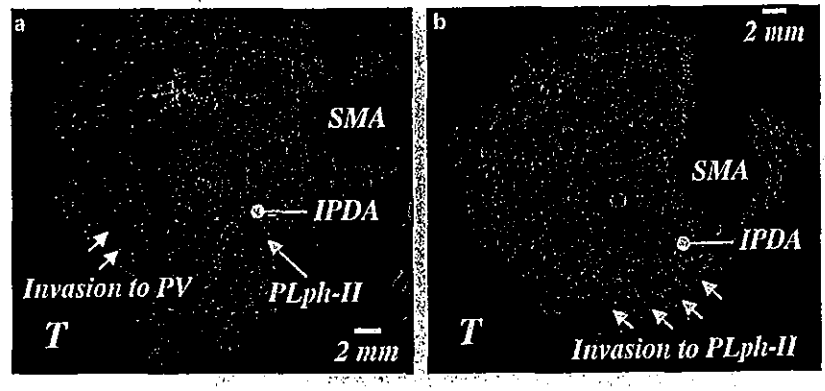


**Fig. 2. a** An intact echogenic area around the IPDA indicates no invasion to PLph-II. Note the portal vein invasion by tumor. **b** Low echoic lesion around the IPDA indicates the invasion to the PLph-II.

cular ultrasound (IVUS) catheter. Sequential observation of the surrounding structures by IPEUS showed that the inferior pancreaticoduodenal artery (IPDA) traverses behind the portal vein and enters the uncinate process of the pancreas. The IPDA exists in the second portion of the PL and the echogenic area around the IPDA between the uncinate process and the SMA corresponds to the second portion of the pancreatic head nerve plexus (PLph-II) (fig. 1a, b). The diagnostic criterion for the PL invasion is, therefore, low echoic infiltration of the area around the IPDA (fig. 2a, b) [8].

The portal vein wall was visualized as an echogenic band with a thickness of 0.5–1.0 mm. The diagnostic criterion for portal venous invasion at IPEUS was obliteration of the echogenic band of the portal venous wall by the hypoechoic mass. There was one observer (T.K.) of the IPEUS finding. Tabulation of the IPEUS findings was performed at the time of surgery.

Statistical analysis was performed by the $\chi^2$ test for group differences, and Student's t test for mean differences using Statview software (Version 5, 1998, SAS Institute, Inc.). Survival rates were calculated by the Kaplan-Meier method, and statistical significance was examined using the log-rank test. The difference was considered significant if the p value was $<0.05$.

## Results

*Patients and Operative Procedures*

There were 43 men and 21 women with a mean age of 61.6 years (range, 43–78 years). Of 64 patients, 48 underwent segmental resection of the portal vein combined with tumor resection. Pancreatoduodenectomy with distal gastrectomy was performed in 32 patients, pylorus-preserving pancreatoduodenectomy in 17, total pancreatectomy in 5 and extended distal pancreatectomy in 10.

*Histopathologic Parameters and Staging*

Histological examination of the surgical specimen confirmed pancreatic adenocarcinoma in all 64 patients who underwent tumor resection. Differentiation was well in 6 patients, moderate in 52 and poor in 5. One patient was diagnosed as adenosquamous carcinoma. Invasion to the duodenum was found in 25 patients (39%) and invasion to the portal vein in 33 (52%). The portal vein invasion was defined as the invasion deep into the adventitia of the portal vein wall by pancreatic carcinoma, which was confirmed histologically. Intrapancreatic nerve invasion was found in the majority of the cases (56 of 64; 88%). The resection margins were tumor free in 43 (67%) and tumor positive in 21 (33%). In most cases (56 of 64), tumor size was found >2 cm. Lymph node invasion was seen in 37 cases (58%). When the patients were stratified according to stage using the TNM classification by UICC, 27 cases had stages I through III tumors. There were several cases in stage IVb in which metastasis to lymph nodes beyond regional level has been defined as distant organ metastasis by UICC.

*IPEUS*

The IPDA was visualized in 61 out of 64 cases. In the other 3 cases, it was not visualized because it traversed behind the portal vein beyond the effective visual field of the IPEUS. There were 18 cases in which PL invasion was confirmed pathologically positive (28%). There was one false-positive case caused by an attenuation of the ultrasound beam around the IPDA due to associated pancreatitis. There was one false-negative case in which the invasion was found at the first portion and the right celiac ganglia, but not at the second portion of the PL. Three poor visibility cases were negative in extrapancreatic nerve plexus invasion. In this study, these 3 cases were regarded as false-positive cases. Consequently, IPEUS showed 94% (17/18) sensitivity, 91% (42/46) specificity, 81% (17/21) positive predictive value, 98% (42/43) negative predictive value and 92.1% (59/64) overall accuracy for the diagnosis of the PL invasion. The diagnostic accuracies of PL invasion by IPEUS in pancreatic cancer which size was

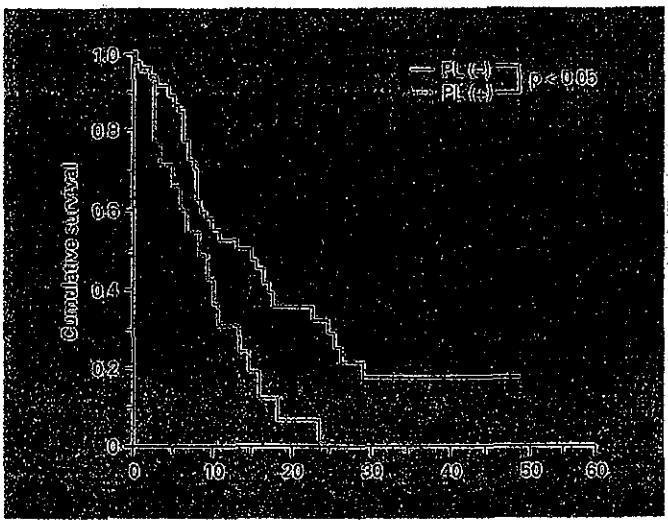


**Fig. 3.** Cumulative survival rates between the patients with or without the PL invasion. The difference was significant by log-rank test ($p < 0.05$).

**Table 1.** Characteristics of patients according to PL status

| PL invasion | Negative (n = 46) | Positive (n = 18) |
|---|---|---|
| Age (mean ± SD)* | 60.8 ± 8.5 | 63.8 ± 6.8 |
| Sex (M/F)* | 31/15 | 12/6 |
| Tumor differentiation* | | |
| Well | 3 | 3 |
| Moderate | 40 | 12 |
| Poor | 2 | 3 |
| Adenosquamous | 1 | – |
| Tumor size (<2 cm/>2 cm)* | 8/38 | 0/18 |
| Lymph node invasion (–/+)* | 22/24 | 5/13 |
| Portal vein invasion (–/+)** | 26/20 | 5/13 |
| Tumor-free/positive margin | 38/8 | 5/13 |
| pTNM stage (I–III/IVa–b)** | 25/21 | 2/16 |
| 1-, 2- and 3-year survival rates, % | 52/32/18 | 31/0/0 |

* There was no statistically significant difference in distribution ($p > 0.05$). ** $p < 0.05$.

larger than 2 cm were described as follows. Sensitivity was 94% (17/18), specificity 92% (35/38), positive predictive value 85% (17/20). Negative predictive value 97% (35/36), and overall accuracy 93% (52/56).

The diagnosis of portal venous invasion could be possible in all cases by IPEUS. Sensitivity, specificity, and overall accuracies of IPEUS were 97% (33/34), 93% (28/30), and 95% (61/64).

*Clinical Significance of the PL Invasion*

To evaluate the clinical significance of the PL invasion, all patients were further grouped according to the PL status (table 1). There was no significant correlation between PL invasion and age, sex, tumor differentiation, tumor size or lymph node metastasis ($p > 0.05$). However, a significant correlation was found between PL invasion and the portal vein invasion ($p = 0.05$), or invasion of the margins ($p < 0.0001$). There was also a significant correlation between PL status and pTNM stage ($p = 0.0039$).

Overall 1-, 2- and 3-year survival for 64 patients was 25.0, 12.0 and 5.0%, with a median survival of 9 months. The 1-, 2- and 3-year survival in 18 patients with PL invasion was 31, 0 and 0% whereas it was 52, 32 and 18% in those 46 patients without PL invasion, and the difference was statistically significant ($p = 0.008$, log-rank test) (fig. 3). As expected, a significant difference in survival after resection was found between patients with tumor-positive or tumor-free margins ($p < 0.001$), and between patients with pTNM stage I–III tumor or IVa,b tumor ($p = 0.0085$). Log-rank survival analysis showed that the worst prognosis was observed for the 20 patients with tumor-positive margins. None of these patients survived 18 months with a mean survival of only 7 months.

## Discussion

Pancreatic carcinoma is an almost uniformly fatal disease and the overall survival rates after resection are only approximately 10%. But surgical resection is only curative therapy for pancreatic carcinoma. In this study, patients for surgery were selected on the basis of preoperative US, CT, and angiography. Obvious liver metastases and splanchnic arterial invasion such as superior mesenteric artery and common hepatic artery were not indicated for resection. Portal vein itself was not the reason of unresectability.

IPEUS can be performed preoperatively by means of a percutaneous transhepatic route. We performed this procedure in biliary tract cancers which require percutaneous transhepatic portal embolization (PTPE). In these cases, we performed IPEUS preoperatively with PTPE [13]. But in pancreatic cancer, we did not perform percutaneous transhepatic portography, so IPEUS was not performed preoperatively. The diagnostic principal behind IPEUS was based on the anatomical relation between pancreas and retroperitoneal nerve plexuses. Yoshioka and Wakabayashi [14], who first studied the pancreatic head nerve

plexus in detail, divided PL into two main portions. The first portion extends from the right celiac ganglia to the upper median margin of the uncinate process of the pancreas, and the second portion extends from the SMA to the median margin of the uncinate process. Other extrapancreatic plexuses have been described around the superior mesenteric artery and celiac artery. The PLph-II is the main site for the invasion by the carcinoma of the pancreatic head [6]. The incidence of PL invasion in carcinoma of the pancreas is reported to be 57–61% [5, 9, 15]. In the current study, IPEUS could detect the most of the PL invasions with high accuracy rate of 97%. In this study, the portal venous invasion rate was 52% (33/64) and extrapancreatic nerve plexus invasion rate was 28% (18/64). Extrapancreatic nerve plexus invasion did not correlate very well with portal vein invasion. Basically, the extrapancreatic nerve plexus invasion cases were accompanied by the portal vein invasion, but not vice versa. So, the portal vein invasion did not predict the extrapancreatic nerve plexus invasion. We reported comparative results of portal venous invasion by pancreatobiliary cancer between IPEUS, CT, and angiography [13]. IPEUS was reported to be superior to CT, and angiography in diagnosis of portal vein invasion. Intraoperative IPEUS can diagnose the PL invasion as well as the portal vein invasion. IPEUS provided the important information to the portal vein resection and reconstruction because the direction and longitudinal distance of the portal vein invasion was accurately diagnosed. Moreover, the accurate diagnosis of the PL invasion with IPEUS navigates the extent of dissection of the nerve plexuses around the SMA to obtain negative dissected margin which closely correlates with prognosis after resection.

Several studies showed that the presence of PL invasion worsens the prognosis of patients with pancreatic carcinoma [4, 7, 16]. The present study revealed that the PL status is significantly associated with the margin status which might be responsible for the dismal prognosis of those cases. Several studies have retrospectively examined margin status [3, 17, 18]. We recently reported that the indication for the portal vein resection is to obtain cancer-free margin and there is no indication for the resection of the tumor if cancer-free margin cannot be obtained by portal vein resection [3]. Trede et al. [19] reported significantly reduced survival rate in patients with margin-positive resection. Willett et al. [17] reported that survival was largely dictated by resection margin. Yeo et al. [18] recently reported that resection margin status along with tumor size, intraoperative blood loss and adjuvant treatment was among the four factors representing independent predictors of outcome. As the data from these studies and the present study indicated, it is concluded that the outcome in patients with a positive margin is dismal. To cure patients with pancreatic cancer, it is important to determine the extent of pancreatic cancer to achieve tumor-free margins with radical operation which includes wide range of lymphadenectomy, retroperitoneal dissection and, when indicated, PV/SMV resection.

The fact that PL invasion is significantly associated with margin status might be explained by the anatomical relation between the PL and the SMA. The distance between the PL and the SMA is actually very close which makes curative resection difficult. Beyond this anatomical approach, there may be several other explanations for that fact. Extrapancreatic nerve plexus invasion is one of the major causes of recurrence of resected pancreatic cancer as tumor cells appear to migrate along the nerve fibers for a long distance and reach the celiac plexus where they form a nidus. There appears to be no relationship between the size of the tumor and the PL invasion since small tumors or even microscopic cancer show invasion to the PL [20, 21]. It is possible that the specific molecules produced by nerve tissue and/or tumor cells take part in the mechanism for neural invasion and therefore the worsened outcome.

When considering surgical treatment of pancreatic cancer, complete dissection of extrapancreatic nerve plexus, especially the second portion of the PL and nerve plexus around the SMA, may be necessary to obtain a tumor-free surgical margin. However, complete resection of the nerve plexus around the SMA causes severe diarrhea after resection. Therefore, IPEUS as a powerful tool for intraoperative diagnosis of the PL invasion is necessary for planning the operative procedure. If a patient has no carcinoma invasion to the second portion of the PL, the left semicircular nerve plexus around the SMA is preserved in order to prevent diarrhea.

According to the present results, the prognosis of the cases with PL invasion is very poor and the indication for resection is doubtful. From this study, we concluded that when extrapancreatic nerve plexus invasion was diagnosed by IPEUS, there was no indication for resection because the prognosis of extrapancreatic nerve invasion cases was considered to be too poor to be resected.


## Acknowledgment

This study was supported by a grant to Dr. E. Tezel from the Japanese Ministry of Education, Science, Sports and Culture.

## References


1 Parker SL, Tong T, Bolden S, Wingo PA: Cancer statistics. CA Cancer J Clin 1996;46:5–27.
2 Yeo CJ, Cameron JL, Lillemoe KD, Sitzmann JV, Hruban RH, Goodman SN, Dooley WC, Coleman J, Pitt HA: Pancreaticoduodenectomy for cancer of the head of the pancreas. 201 cases. Ann Surg 1995;221:721–731.
3 Nakao A, Kaneko T, Takeda S, Inoue S, Harada A, Nomoto S, Ekmel T, Yamashita K, Hatsuno T: The role of extended radical operation for pancreatic cancer. Hepatogastroenterology 2001;48:949–952.
4 Nakao A, Harada A, Nonami T, Kaneko T, Takagi H: Clinical significance of carcinoma invasion of the extrapancreatic nerve plexus in pancreatic cancer. Pancreas 1996;12:357–361.
5 Kayahara M, Nagakawa T, Konishi I, Ueno K, Ohto T, Miyazaki I: Clinicopathological study of pancreatic carcinoma with particular reference to the invasion of the extrapancratic neural plexus. Int J Pancreatol 1991;10:105–111.
6 Nagakawa T, Kayahara M, Ohta T, Ueno K, Konishi I, Miyazaki I: Patterns of neural and plexus invasion of human pancratic cancer and experimental cancer. Int J Pancreatol 1991;10: 113–119.
7 Nagakawa T, Mori K, Nakano T, Kadoya M, Kobayashi H, Akiyama T, Kayahara M, Ohta T, Ueno K, Higashino Y, Konishi I, Miyazaki I: Perineural invasion of carcinoma of the pancreas and biliary tract. Br J Surg 1993;80:619–621.
8 Kaneko T, Kimata H, Sugimoto H, Inoue S, Ito S, Ishiguchi T, Nakao A: Power Doppler ultrasonography for the assessment of vascular invasion by pancreatic cancer. Pancreatology 2002; 2:61–68.
9 Kaneko T, Nakao A, Inoue S, Nomoto S, Nagasaka T, Nakashima N, Harada A, Nonami T, Takagi H: Extrapancreatic nerve plexus invasion by carcinoma of the head of the pancreas. Diagnosis with intraportal endovascular ultrasonography. Int J Pancreatol 1996;19:1–7.
10 Kaneko T, Nakao A, Takagi H: Intraportal endovascular ultrasonography for pancreatic cancer. Semin Surg Oncol 1998;15:47–51.
11 Japan Pancreas Society: Classification of pancreatic carcinoma. First English Edition. Tokyo, Kanehara Publishing, 1996.
12 Sobin LH, Wittekind Ch: TNM Classification of Malignant Tumours, ed 5. New York, Wiley-Liss, 1997.
13 Kaneko T, Nakao A, Inoue S, Harada A, Nonami T, Ito S, Endo T, Takagi H: Intraportal endovascular ultrasonography in the diagnosis of portal vein invasion by pancreatobiliary carcinoma. Ann Surg 1995;222:711–718.
14 Yoshioka H, Wakabayashi T: Therapeutic neurotomy on head of pancreas for relief of pain due to chronic pancreatitis. Arch Surg 1958;76: 546–554.
15 Matsuda M, Nimura Y: Perineural invasion in carcinoma of the head of the pancreas (abstract in English). Jpn J Surg 1983;84:719–728.
16 Tezel E, Hibi K, Nagasaka T, Nakao A: PGP9.5 as a prognostic factor in pancreatic cancer. Clin Cancer Res 2001;6:4764–4767.
17 Willett CG, Lewandrowski K, Warshaw AL, Efird J, Compton CC: Resection margins in carcinoma of the head of the pancreas. Implications for radiation therapy. Ann Surg 1993; 217:144–148.
18 Yeo CJ, Abrams RA, Grochow LB, Sohn TA, Ord SE, Hruban RH, Zahurak ML, Dooley WC, Coleman J, Sauter PK, Pitt HA, Lillemoe KD, Cameron JL: Pancreaticoduodenectomy for pancreatic carcinoma: postoperative adjuvant chemoradiation improves survival. A prospective, single-institution experience. Ann Surg 1997;225:621–636.
19 Trede M, Schwall G, Saeger HD: Survival after pancreatoduodenectomy. 118 consecutive resections without an operative mortality. Ann Surg 1990;211:447–458.
20 Nagai H, Kuroda A, Morioka Y: Lymphatic and local spread of T1 and T2 pancreatic cancer: A study of autopsy material. Ann Surg 1986;204:65–71.
21 Kimura W, Morikane K, Esaki Y, Chan WC, Pour PM: Histologic and biologic patterns of microscopic pancreatic ductal adenocarcinomas detected incidentally at autopsy. Cancer 1998;82:1839–1849.

# Frequent promoter methylation and gene silencing of *CDH13* in pancreatic cancer

Mitsuru Sakai, Kenji Hibi,[1] Katsumi Koshikawa, Soichiro Inoue, Shin Takeda, Tetsuya Kaneko and Akimasa Nakao

Department of Surgery II, Nagoya University School of Medicine, 65 Tsurumai-cho, Showa-ku, Nagoya 466-8560

(Received April 2, 2004/Revised May 10, 2004/Accepted May 10, 2004)

**It has recently been reported that *CDH13* expression is silenced by aberrant methylation of the promoter region in several cancers. We examined the methylation status of the *CDH13* gene in pancreatic cancer using methylation-specific PCR (MSP), and detected aberrant methylation of *CDH13* in all 6 pancreatic cancer cell lines examined. To confirm the status of the *CDH13* gene in relation to the methylation pattern, we next examined *CDH13* expression in these cell lines using reverse transcription (RT)-PCR. As expected, no *CDH13* expression was detected in any of the 6 pancreatic cancer cell lines. Moreover, 5-aza-2′-deoxycytidine (5-aza-dC) treatment of *CDH13*-methylated cell lines led to restoration of *CDH13* expression. Among primary pancreatic cancers, 19 of 33 (58%) cases exhibited *CDH13* methylation, while no cases exhibited it in corresponding normal pancreatic tissues. *CDH13* methylation was detected even in relatively early pancreatic cancers, such as stage II cancers and cancers less than 2 cm in diameter. Our results suggest that the aberrant methylation of *CDH13* occurs frequently in pancreatic cancer, even at a relatively early stage. (Cancer Sci 2004; 95: 588–591)**

Pancreatic cancer is one of the most aggressive cancers, and is the fifth leading cause of cancer mortality in the Western population.[1] The prognosis is poor, and 5-year survival is rare.[2] Pancreatic carcinogenesis is a multi-stage process resulting from the accumulation of genetic changes in the somatic DNA of normal cells.[3] Mutations in proto-oncogenes such as *K-ras* and tumor suppressor genes such as *p16*, *p53*, and *DPC4* are well known.[4–7] The accumulation of these genetic changes leads to a profound disturbance in cell cycle regulation and normal growth. However, further studies of the genetic alterations are needed to clarify fully the biological character of pancreatic cancer.

In recent years, there has been increasing interest in a large family of transmembrane glycoproteins, the cadherins. Cadherins are prime mediators of calcium-dependent cell-cell adhesion in normal cells and are also involved in contact inhibition of cell growth by inducing cell cycle arrest.[8,9] Loss of their expression has been described in many epithelial cancers and may play a role in tumor cell invasion and metastasis.[10,11] Recently, aberrant methylation of the *CDH13* (*H-cadherin*) gene associated with gene silencing has been reported in several primary tumors including breast, lung, colorectal, and ovarian cancers, and myeloid leukemia.[12–16] These reports suggested that *CDH13* may be an important gene for the progression of cancer and prompted us to examine *CDH13* status in pancreatic cancer.

In this study, we first examined the methylation status and gene expression of *CDH13* in pancreatic cancer cell lines using methylation-specific PCR (MSP) and reverse transcription-PCR (RT-PCR), respectively. We then examined the methylation status of the *CDH13* gene in primary pancreatic cancers and corresponding normal pancreatic tissues derived from 33 patients, and evaluated the correlation between the methylation status and the clinicopathological findings.

## Materials and Methods

**Sample collection and DNA preparation.** Six pancreatic cancer cell lines (AsPC-1, BxPC-3, Capan-1, Capan-2, MIA PaCa-2, and SW1990) and 1 colorectal cancer cell line (SW480) were obtained from American Type Culture Collection (Manassas, VA). They were grown in RPMI 1640 supplemented with 10% fetal bovine serum and incubated in 5% $CO_2$ at 37°C.

Thirty-three primary tumors and corresponding nonmalignant pancreatic tissues were collected at the Nagoya University School of Medicine from pancreatic cancer patients who had been diagnosed histopathologically. All pancreatic cancers were invasive ductal carcinomas. These samples were obtained during surgery. Written informed consent, as required by the institutional review board, was obtained from all patients. All samples were quickly frozen in liquid nitrogen and stored at −80°C until analysis. Genomic DNA was obtained from these samples by digestion with proteinase K, followed by phenol/chloroform extraction as described previously.[17]

**Bisulfite modification and MSP.** DNA from tumor and normal specimens was subjected to bisulfite treatment as described previously.[18] Briefly, 2 μg of DNA was denatured with NaOH and modified with sodium bisulfite. DNA samples were then purified using the Wizard purification resin (Promega Corp., Madison, WI), treated again with NaOH, precipitated with ethanol, and resuspended in water. The modified DNA was used as a template for MSP. Primer sequences of CDH13 for the unmethylated reaction were: CDH13 UMS (sense), 5′-TTGTGGGGT-TGTTTTTTGT-3′, and CDH13 UMAS (antisense), 5′-AACTTTTCATTCATACACACA-3′, which amplify a 242-base pair product. Primer sequences of CDH13 for the methylated reaction were: CDH13 MS (sense), 5′-TCGCGGGGT-TCGTTTTTCGC-3′, and CDH13 MAS (antisense), 5′-GACGTTTTCATTCATACACGCG-3′, which amplify a 243-base pair product. These primer sequences were described previously.[14,19] The PCR amplification of modified DNA samples consisted of 1 cycle of 95°C for 5 min; 1 cycle of 78°C for 10 min, 30 cycles of denaturing at 95°C for 30 s, 1 min of annealing at specific temperature, 1 min of extension at 72°C and a final extension step of 10 min at 72°C. Modified DNAs obtained from SW480 and Capan-1 were used as positive controls for unmethylated and methylated alleles, respectively. Controls without DNA were included in each assay. Ten microliters of each PCR product was loaded directly onto nondenaturing 6% polyacrylamide gels, stained with ethidium bromide, and visualized under UV illumination. Each MSP was repeated at least twice.

**RT-PCR.** Expression of the *CDH13* gene was analyzed by RT-PCR. Total RNA was extracted from pancreatic and colorectal cancer cell lines with "ISOGEN" (Nippon Gene, Tokyo) following the manufacturer's instructions. First-strand cDNA was generated from RNA as described previously.[20] cDNA was amplified by means of a primer set that was specific for the

[1]To whom correspondence should be addressed.
E-mail: khibi@med.nagoya-u.ac.jp

*CDH13* gene. Primer sequences were: CDH13 S (sense), 5′-TTCAGCAGAAAGTGTTCCATAT-3′, and CDH13 AS (antisense), 5′-GTGCATGGACGAACAGAGT-3′. The PCR amplification consisted of 1 cycle of 94°C for 2 min; 33 cycles of 94°C for 30 s, 57°C for 30 s, and 72°C for 30 s; and 1 cycle of 72°C for 5 min. Expression of β-actin was used as a control to confirm the success of the RT reaction. PCR products were visualized on 2% agarose gels stained with ethidium bromide.

**5-Aza-2′-deoxycytidine (5-aza-dC) treatment.** Methylated cell lines of pancreatic cancer were treated with 5-aza-dC (Sigma-Aldrich, St. Louis, MO), a demethylating agent. Cells ($1.5\times10^6$) were grown for 6 days in the presence of different concentrations of 5-aza-dC (0, 1, 3, and 10 μ*M*), with medium changes on days 1, 3, and 5.

**Statistical analysis.** The associations between *CDH13* promoter methylation and clinicopathological parameters were analyzed by using Fisher's exact test.

## Results

We first examined the methylation status of the *CDH13* promoter in 6 pancreatic cancer cell lines using the MSP technique. Aberrant methylation of *CDH13* was detected in all 6 cell lines (Fig. 1A). To confirm the status of the *CDH13* gene according to the methylation pattern, we next examined *CDH13* expression in these cell lines using RT-PCR. As expected, no *CDH13* expression was detected in any of the 6 pancreatic cancer cell lines, whereas *CDH13* expression was distinctly detected in a colorectal cancer cell line (SW480) with unmethylated *CDH13* promoter (Fig. 1B).

To confirm that the promoter methylation was responsible for silencing of the *CDH13* expression, we treated methylated pancreatic cancer cell lines with different concentrations of 5-aza-dC (0, 1, 3, 10 μ*M*), a demethylating agent, and examined *CDH13* expression by RT-PCR. *CDH13* expression in all cell lines was restored in a dosage-dependent manner by the 5-aza-dC treatment (Fig. 1C).

Subsequently, we examined the methylation status of the *CDH13* promoter in primary pancreatic cancers and corresponding normal tissues. Aberrant methylation of the *CDH13* gene was detected in 19 of 33 (58%) primary pancreatic cancers, but not in the corresponding normal pancreatic tissues (Fig. 2). We also examined the methylation status of the *CDH13* gene in 24 primary hepatocellular carcinomas. In contrast to the frequent methylation detected in pancreatic cancer, no aberrant methylation of the *CDH13* gene was detected in these hepatocellular carcinomas (data not shown).

Table 1 shows the *CDH13* methylation status and the clinicopathological findings in 33 pancreatic cancer patients. The *CDH13* methylation was detected even in relatively early pancreatic cancers such as stage II cancers and cancers less than 2 cm in diameter. We then examined the correlation between the *CDH13* methylation status and the clinicopathological findings (Table 2). We found no significant correlation between aberrant methylation in the primary tumors and age, sex, tumor size, histological type, presence of lymph node involvement, stage of the disease, serum CA19-9 level, perineural invasion, venous invasion, or lymphatic invasion.

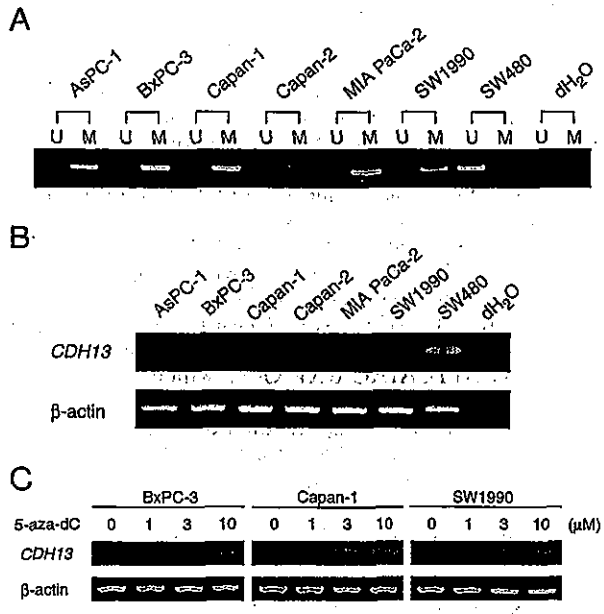


**Fig. 1.** Methylation and expression status of *CDH13* in pancreatic cancer cell lines. (A) MSP of *CDH13* promoter. The presence of a visible PCR product in lanes U indicates the presence of unmethylated genes; the presence of product in lanes M indicates the presence of methylated genes. All 6 pancreatic cancer cell lines show *CDH13* promoter methylation, whereas a colorectal cancer cell line (SW480) has unmethylated *CDH13* promoter. (B) Analysis of *CDH13* expression by RT-PCR. No *CDH13* expression was detected in any of the pancreatic cancer cell lines, whereas *CDH13* expression was distinctly detected in the case of SW480, whose *CDH13* promoter is unmethylated. Expression of β-actin was used as a control to confirm the success of the RT reaction. (C) The effect of 5-aza-2′-deoxycytidine (5-aza-dC) treatment on *CDH13* expression in pancreatic cancer cell lines with methylation of *CDH13* promoter. Recovery of *CDH13* expression was restored dosage-dependently by 5-aza-dC treatment.

## Discussion

Aberrant methylation of the promoter regions associated with gene silencing is one of the major mechanisms for the inactivation of tumor suppressor genes, and has been observed in various cancers,[21] including pancreatic cancer.[22–24] Ueki *et al.* examined the methylation status of several tumor suppressor genes in pancreatic cancer using MSP and defined the "CpG island methylator phenotype (CIMP)" in this disease.[25] CIMP+ phenotype was observed in 14% of pancreatic cancers and aberrant methylation of tumor suppressor genes, such as *RAR*b, *p16*, and *E-cadherin*, appeared at a rate of 5–20% for each gene. These results suggested that aberrant methylation might be a common mechanism for the inactivation of the tumor suppressor gene in pancreatic cancer.

Recently, the *CDH13* gene has been identified as a new member of the cadherin superfamily. Furthermore, it has been reported that *CDH13* gene expression was silenced by aberrant methylation of the promoter region in several primary tumors.[12–16] However, the methylation status of the *CDH13* gene has not yet been studied in pancreatic cancer. In the present study, we examined the methylation status of the *CDH13* gene and found that the *CDH13* promoter was methylated in all 6 pancreatic cancer cell lines and in 19 of 33 primary pancreatic cancers (58%). This result suggests that *CDH13* promoter methylation is a fairly frequent event, and that it plays a role in the progression of pancreatic cancers. *CDH13*, as a member of the cadherin family, would be a cell

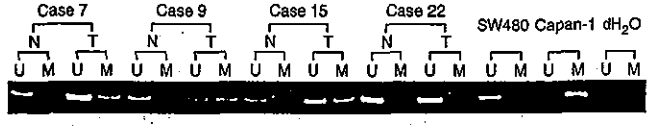


**Fig. 2.** Representative MSP of *CDH13* promoter in primary pancreatic cancers and the corresponding normal tissues. In primary pancreatic cancers, cases 7, 9, and 15 exhibited *CDH13* promoter methylation.

Table 1. *CDH13* methylation status and clinicopathological findings in 33 pancreatic cancer patients

| Case No. | Age | Sex | Tumor size (mm) | Histological type[1] | Lymph node metastasis | TNM stage[2] | CA19-9 (U/ml) | Perineural invasion[3] | Venous invasion[3] | Lymphatic invasion[3] |
|---|---|---|---|---|---|---|---|---|---|---|
| Methylated cases for CDH13 | | | | | | | | | | |
| 1 | 66 | male | 35 | poor | – | II | 90 | – | – | + |
| 5 | 66 | female | 20 | uncertain | – | II | 180 | – | – | – |
| 6 | 83 | female | 45 | well | – | IVA | 3302 | – | – | – |
| 7 | 76 | male | 25 | mod | – | II | 492 | + | – | + |
| 8 | 73 | female | 40 | well | + | IVB | 1476 | + | – | + |
| 9 | 68 | male | 45 | mod | + | IVA | 263 | – | + | + |
| 11 | 52 | male | 45 | mod | + | IVB | <5 | + | + | + |
| 12 | 61 | male | 55 | mod | + | IVA | 3805 | + | + | + |
| 15 | 47 | male | 15 | mod | – | IVA | unknown | + | – | + |
| 17 | 58 | male | 45 | poor | + | IVB | 186 | + | – | + |
| 19 | 63 | male | 45 | mod | + | IVA | 1663 | + | – | + |
| 21 | 66 | male | 70 | poor | + | IVA | 83 | + | + | + |
| 23 | 55 | female | 70 | mod | + | IVA | unknown | + | – | + |
| 26 | 67 | female | 30 | poor | – | IVA | 899 | + | + | + |
| 27 | 58 | male | 30 | mod | + | IVB | 35 | + | + | + |
| 28 | 68 | male | 20 | well | + | III | 104 | – | + | + |
| 29 | 79 | female | 31 | mod | – | II | 34 | + | – | + |
| 31 | 66 | female | 61 | well | + | IVA | 1030 | – | – | – |
| 33 | 69 | male | 30 | mod | + | III | 28 | – | + | + |
| Unmethylated cases for CDH13 | | | | | | | | | | |
| 2 | 51 | female | 35 | mod | – | IVA | 1220 | + | – | – |
| 3 | 68 | male | 30 | mod | + | IVA | 216 | + | + | + |
| 4 | 63 | female | 30 | mod | + | III | 9 | – | – | – |
| 10 | 71 | female | 30 | mod | + | IVA | 1101 | + | – | + |
| 13 | 71 | male | 30 | poor | + | III | 40 | – | – | + |
| 14 | 48 | female | 45 | mod | + | IVA | 126 | + | – | + |
| 16 | 76 | male | 45 | mod | + | IVB | 2149 | + | – | + |
| 18 | 57 | male | 45 | mod | + | IVB | 210 | + | – | + |
| 20 | 62 | male | 18 | mod | – | II | 91 | + | – | + |
| 22 | 50 | female | 20 | mod | + | IVA | 407 | + | – | + |
| 24 | 66 | female | 28 | uncertain | + | IVA | 285 | – | – | + |
| 25 | 71 | female | 18 | mod | – | IVA | 7 | + | + | – |
| 30 | 48 | male | 25 | well | + | III | 24 | – | – | + |
| 32 | 73 | male | 25 | poor | + | IVA | 279 | + | – | + |

1) Well, well differentiated adenocarcinoma; mod, moderately differentiated adenocarcinoma; poor, poorly differentiated adenocarcinoma.
2) Classified according to the International Union Against Cancer tumor-node-metastasis classification.
3) Classified according to the classification of pancreatic carcinoma of the Japan Pancreas Society.

surface glycoprotein responsible for cell adhesion. Therefore, it is conceivable that *CDH13* is inactivated in pancreatic cancers by promoter methylation, leading to cancer cell disassociation, which is a characteristic of pancreatic cancer. Recently, it was reported that *E-cadherin* expression in pancreatic tumor cells resulted in arrest of tumor development at the adenoma stage, whereas expression of a dominant negative form of *E-cadherin* induced early invasion and metastasis.[26] This report supports the notion that the inactivation of cadherin family genes would be a critical event in scattering cancer cells, because they code for proteins responsible for selective cell recognition and adhesion.

In conclusion, our results suggest that the aberrant methylation of *CDH13* occurs frequently in pancreatic cancer, even at a relatively early stage. On the other hand, because of frequent hypermethylation of the *CDH13* gene and the high sensitivity of MSP, which can detect 1 methylated allele among 1000 unmethylated alleles,[27] it can potentially be used for early detection and monitoring of pancreatic cancer by the detection of the *CDH13* methylation status in clinical samples such as serum, stool, pancreatic juice, and duodenal fluid.[18, 28, 29]

We thank Y. Nishikawa and M. Taguchi for their technical assistance.

1. Jemal A, Thomas A, Murray T, Thun M. Cancer statistics, 2002. *CA Cancer J Clin* 2002; 52: 23–47.
2. Rosewicz S, Wiedenmann B. Pancreatic carcinoma. *Lancet* 1997; 349: 485–9.
3. Schneider G, Schmid RM. Genetic alterations in pancreatic carcinoma. *Mol Cancer* 2003; 2: 15.
4. Hruban RH, van Mansfeld AD, Offerhaus GJ, van Weering DH, Allison DC, Goodman SN, Kensler TW, Bose KK, Cameron JL, Bos JL. K-ras oncogene activation in adenocarcinoma of the human pancreas. A study of 82 carcinomas using a combination of mutant-enriched polymerase chain reaction analysis and allele-specific oligonucleotide hybridization. *Am J Pathol* 1993; 143: 545–54.
5. Kalthoff H, Schmiegel W, Roeder C, Kasche D, Schmidt A, Lauer G, Thiele HG, Honold G, Pantel K, Riethmuller G. p53 and K-RAS alterations in pancreatic epithelial cell lesions. *Oncogene* 1993; 8: 289–98.
6. Wilentz RE, Geradts J, Maynard R, Offerhaus GJ, Kang M, Goggins M, Yeo CJ, Kern SE, Hruban RH. Inactivation of the p16 (INK4A) tumor-suppressor gene in pancreatic duct lesions: loss of intranuclear expression. *Cancer Res* 1998; 58: 4740–4.
7. Hahn SA, Schutte M, Hoque AT, Moskaluk CA, da Costa LT, Rozenblum E, Weinstein CL, Fischer A, Yeo CJ, Hruban RH, Kern SE. DPC4, a candidate tumor suppressor gene at human chromosome 18q21.1. *Science* 1996; 271:

Table 2. Correlation between *CDH13* methylation and clinicopathological findings in 33 pancreatic cancer patients

| Clinicopathological findings | Variable | Number of cases | *CDH13* methylation [number (%)] | | *P* value[1] |
|---|---|---|---|---|---|
| | | | Methylated (*n*=19) | unmethylated (*n*=14) | |
| Age | <60 | 10 | 5 (26) | 5 (36) | 0.707 |
| | ≥60 | 23 | 14 (74) | 9 (64) | |
| Sex | male | 19 | 12 (63) | 7 (50) | 0.497 |
| | female | 14 | 7 (37) | 7 (50) | |
| Tumor size | <3cm | 10 | 4 (21) | 6 (43) | 0.257 |
| | ≥3cm | 23 | 15 (79) | 8 (57) | |
| Histological type[2] | well-mod | 25 | 14 (78) | 11 (85) | >0.999 |
| | poor | 6 | 4 (22) | 2 (15) | |
| Lymph node metastasis | – | 10 | 7 (37) | 3 (21) | 0.455 |
| | + | 23 | 12 (63) | 11 (79) | |
| TNM stage[3] | I, II, III | 10 | 6 (32) | 4 (29) | >0.999 |
| | IVA, IVB | 23 | 13 (68) | 10 (71) | |
| CA19-9 level (U/ml) | <100 | 11 | 6 (35) | 5 (36) | >0.999 |
| | ≥100 | 20 | 11 (65) | 9 (64) | |
| Perineural invasion[4] | – | 11 | 7 (37) | 4 (29) | 0.719 |
| | + | 22 | 12 (63) | 10 (71) | |
| Venous invasion[4] | – | 23 | 11 (58) | 12 (86) | 0.131 |
| | + | 10 | 8 (42) | 2 (14) | |
| Lymphatic invasion[4] | – | 6 | 3 (16) | 3 (21) | >0.999 |
| | + | 27 | 16 (84) | 11 (79) | |

1) Analyzed by Fisher's exact test.
2) Well-mod, well or moderately differentiated adenocarcinoma; poor, poorly differentiated adenocarcinoma.
3) Classified according to the International Union Against Cancer tumor-node-metastasis classification.
4) Classified according to the classification of pancreatic carcinoma of the Japan Pancreas Society.


350–3.
8. Takeichi M. Cadherin cell adhesion receptors as a morphogenetic regulator. *Science* 1991; **251**: 1451–5.
9. Levenberg S, Yarden A, Kam Z, Geiger B. p27 is involved in N-cadherin-mediated contact inhibition of cell growth and S-phase entry. *Oncogene* 1999; **18**: 869–76.
10. Takeichi M. Cadherins in cancer: implications for invasion and metastasis. *Curr Opin Cell Biol* 1993; **5**: 806–11.
11. Behrens J. The role of cell adhesion molecules in cancer invasion and metastasis. *Breast Cancer Res Treat* 1993; **24**: 175–84.
12. Lee SW. H-Cadherin, a novel cadherin with growth inhibitory functions and diminished expression in human breast cancer. *Nat Med* 1996; **2**: 776–82.
13. Toyooka KO, Toyooka S, Virmani AK, Sathyanarayana UG, Euhus DM, Gilcrease M, Minna JD, Gazdar AF. Loss of expression and aberrant methylation of the *CDH13* (H-cadherin) gene in breast and lung carcinomas. *Cancer Res* 2001; **61**: 4556–60.
14. Toyooka S, Toyooka KO, Harada K, Miyajima K, Makarla P, Sathyanarayana UG, Yin J, Sato F, Shivapurkar N, Meltzer SJ, Gazdar AF. Aberrant methylation of the *CDH13* (H-cadherin) promoter region in colorectal cancers and adenomas. *Cancer Res* 2002; **62**: 3382–6.
15. Kawakami M, Staub J, Cliby W, Hartmann L, Smith DI, Shridhar V. Involvement of H-cadherin (*CDH13*) on 16q in the region of frequent deletion in ovarian cancer. *Int J Oncol* 1999; **15**: 715–20.
16. Roman-Gomez J, Castillejo JA, Jimenez A, Cervantes F, Boque C, Hermosin L, Leon A, Granena A, Colomer D, Heiniger A, Torres A. Cadherin-13, a mediator of calcium-dependent cell-cell adhesion, is silenced by methylation in chronic myeloid leukemia and correlates with pretreatment risk profile and cytogenetic response to interferon alfa. *J Clin Oncol* 2003; **21**: 1472–9.
17. Hibi K, Robinson CR, Booker S, Wu L, Hamilton SR, Sidransky D, Jen J. Molecular detection of genetic alterations in the serum of colorectal cancer patients. *Cancer Res* 1998; **58**: 1405–7.
18. Hibi K, Taguchi M, Nakayama H, Takase T, Kasai Y, Ito K, Akiyama S, Nakao A. Molecular detection of p16 promoter methylation in the serum of patients with esophageal squamous cell carcinoma. *Clin Cancer Res* 2001; **7**: 3135–8.
19. Sato M, Mori Y, Sakurada A, Fujimura S, Horii A. The H-cadherin (CDH13) gene is inactivated in human lung cancer. *Hum Genet* 1998; **103**: 96–101.
20. Hibi K, Takahashi T, Sekido Y, Ueda R, Hida T, Ariyoshi Y, Takagi H, Takahashi T. Coexpression of the stem cell factor and the c-kit genes in small-cell lung cancer. *Oncogene* 1991; **6**: 2291–6.
21. Merlo A, Herman JG, Mao L, Lee DJ, Gabrielson E, Burger PC, Baylin SB, Sidransky D. 5′ CpG island methylation is associated with transcriptional silencing of the tumour suppressor p16/CDKN2/MTS1 in human cancers. *Nat Med* 1995; **1**: 686–92.
22. Dammann R, Schagdarsurengin U, Liu L, Otto N, Gimm O, Dralle H, Boehm BO, Pfeifer GP, Hoang-Vu C. Frequent RASSF1A promoter hypermethylation and K-ras mutations in pancreatic carcinoma. *Oncogene* 2003; **22**: 3806–12.
23. Fukushima N, Sato N, Ueki T, Rosty C, Walter KM, Wilentz RE, Yeo CJ, Hruban RH, Goggins M. Aberrant methylation of preproenkephalin and p16 genes in pancreatic intraepithelial neoplasia and pancreatic ductal adenocarcinoma. *Am J Pathol* 2002; **160**: 1573–81.
24. Fukushima N, Sato N, Sahin F, Su GH, Hruban RH, Goggins M. Aberrant methylation of suppressor of cytokine signalling-1 (SOCS-1) gene in pancreatic ductal neoplasms. *Br J Cancer* 2003; **89**: 338–43.
25. Ueki T, Toyota M, Sohn T, Yeo CJ, Issa JP, Hruban RH, Goggins M. Hypermethylation of multiple genes in pancreatic adenocarcinoma. *Cancer Res* 2000; **60**: 1835–9.
26. Perl AK, Wilgenbus P, Dahl U, Semb H, Christofori G. A causal role for E-cadherin in the transition from adenoma to carcinoma. *Nature* 1998; **392**: 190–3.
27. Herman JG, Graff JR, Myohanen S, Nelkin BD, Baylin SB. Methylation-specific PCR: a novel PCR assay for methylation status of CpG islands. *Proc Natl Acad Sci USA* 1996; **93**: 9821–6.
28. Nakayama H, Hibi K, Takase T, Yamazaki T, Kasai Y, Ito K, Akiyama S, Nakao A. Molecular detection of p16 promoter methylation in the serum of recurrent colorectal cancer patients. *Int J Cancer* 2003; **105**: 491–3.
29. Klump B, Hsieh CJ, Nehls O, Dette S, Holzmann K, Kiesslich R, Jung M, Sinn U, Ortner M, Porschen R, Gregor M. Methylation status of p14ARF and p16INK4a as detected in pancreatic secretions. *Br J Cancer* 2003; **88**: 217–22.

Available online at www.sciencedirect.com
SCIENCE DIRECT®
Biochemical and Biophysical Research Communications 315 (2004) 85–92
BBRC
www.elsevier.com/locate/ybbrc

# Metastin and its variant forms suppress migration of pancreatic cancer cells

Toshihiko Masui,[a] Ryuichiro Doi,[a,*] Tomohiko Mori,[a] Eiji Toyoda,[a] Masayuki Koizumi,[a] Kazuhiro Kami,[a] Daisuke Ito,[a] Stephen C. Peiper,[b] James R. Broach,[c] Shinya Oishi,[d] Ayumu Niida,[d] Nobutaka Fujii,[d] and Masayuki Imamura[a]

[a] *Department of Surgery and Surgical Basic Science, Kyoto University, Kyoto, Japan*
[b] *Department of Pathology, Medical College of Georgia, USA*
[c] *Department of Molecular Biology, Princeton University, USA*
[d] *Department of Bioorganic Medicinal Chemistry, Kyoto University, Kyoto, Japan*

Received 28 December 2003

**Abstract**

Metastin, a post-translationally modified variant of KiSS1, was recently identified as an endogenous peptide agonist for a novel G-protein coupled receptor, hOT7T175 (AXOR12, GPR54). In this study, we analyzed the role of KiSS1 and hOT7T175 in both pancreatic cancer tissues and pancreatic cancer cell lines. Furthermore, we synthesized novel short variant forms of metastin and tested the inhibitory effect of those variants on in vitro cell functions that are relevant to metastasis. Pancreatic cancer tissues showed significantly lower expression of KiSS1 mRNA than normal tissues ($p = 0.018$), while cancer tissues showed significantly higher expression of hOT7T175 mRNA than normal pancreatic tissues ($p = 0.027$). In human pancreatic cancer cell lines, KiSS1 mRNA was highly expressed in 2 out of 6 pancreatic cancer cell lines, while hOT7T175 mRNA was expressed in all cell lines at various degrees. PANC-1 cells showed the highest expression of hOT7T175. Exogenous metastin did not suppress cell proliferation but significantly reduced the in vitro migration of PANC-1 cells ($p < 0.01$). Metastin induced activation of ERK1 in PANC-1 and AsPC-1 cells. Finally, we synthesized 3 novel short variant forms of metastin, FM053a2TFA, FM059a2TFA, and FM052a4TFA. These metastin variants significantly suppressed the migration of PANC-1 cells and activated ERK1. These data suggest that the metastin receptor, hOT7T175, is one of the promising targets for suppression of metastasis, and that small metastin variants could be an anti-metastatic agent to pancreatic cancer.


*Keywords:* KiSS1; hOT7T175; Metastin; Pancreatic cancer; Migration; Metastasis

The KiSS1 peptide was originally identified as being differentially up-regulated in C8161 melanoma cells that have been rendered to have non-metastatic function by microcell mediated transfer of human chromosome 6 [1]. Transfection of *KiSS1* into human melanoma and breast carcinoma cells prevents these cells from metastasizing without an effect on cell proliferation [2]. Furthermore, the KiSS1 product has been shown to repress 92-kDa type 4 collagenase (MMP-9) expression by affecting NF-κB binding to the promoter [3]. The KiSS1 product was found to be expressed in normal human placenta, testis, brain, pancreas, and liver [4].

Recently, it was shown that the human metastasis suppressor gene *KiSS1* encodes a COOH-terminally amidated peptide with 54 amino acid residues, and that this peptide is a ligand of a novel human G-protein coupled receptor (AXOR12 and hOT7T175) which couples primarily to Gq/11 [4–7]. The receptor has a high degree of homology (81% amino acid identity) to the rat orphan heptahelical receptor, GPR54 [8], indicating that these two receptors are orthologs. The peptide ligand, named as metastin, enhances the expression and activity of focal adhesion kinase, and attenuates pulmonary metastasis of hOT7T175 transfected

* Corresponding author. Fax: +81-75-751-4390.
*E-mail address:* doir@kuhp.kyoto-u.ac.jp (R. Doi).

0006-291X/$ - see front matter © 2004 Elsevier Inc. All rights reserved.
doi:10.1016/j.bbrc.2004.01.021

B16-BL6 melanomas in vivo [5]. In another experiment, metastin inhibits chemotaxis and invasion of hOT7T175 transfected Chinese hamster ovary cells (CHO cells) in vitro with the activation of phospholipase C, arachidonic acid release, and phosphorylation of ERK [6,7]. These indicate that metastin-hOT7T175 axis may act as an anti-metastatic system. The characteristics of inhibitory effects on cancer cell metastasis without affecting cellular growth properties of normal cells make the metastin receptor to be an attractive target for cancer therapy.

The *KiSS1* is located on human chromosome1q32–q41 [9]. However, evidences from subsequent experiments suggest that the expression of *KiSS1* is regulated by a gene(s) located in the region between 6q16.3 and q23 [1]. In pancreatic cancer, losses of 6q, 8p, 9p, 17p, and 18q are frequently observed and those alterations tend to cause lymph node and distant metastases, which suggests a suppressor gene(s) important for pancreatic cancer metastasis may exist in these regions [10–12]. Therefore, pancreatic cancer, has good reasons to downregulate KiSS1 expression. Moreover, in other cancers such as ovarian cancer, breast cancer, and thyroid papillary cancer, over-expression of hOT7T175 has been demonstrated, although KiSS1 is less frequently expressed in the tumor tissue [4,5]. Until now, however, expressions of KiSS1 and hOT7T175, and their function have not been investigated in pancreatic cancer. The purpose of the present study was to determine if KiSS1 and its receptor hOT7T175 are expressed in pancreatic cancer tissues, and to analyze the effect of exogenous metastin on pancreatic cancer cell lines with different expression levels of hOT7T175. Finally, we newly synthesized short variant forms of metastin and tested the inhibitory effect of those variants on in vitro cell functions that are relevant to metastasis.

## Materials and methods

*Cell culture.* Pancreatic cancer cell lines, AsPC-1, BxPC-3, Capan-2, CFPAC-1, PANC-1, and SUIT-2 were purchased from the American Type Culture Collection. Cells were cultured as monolayers in the appropriate medium supplemented with 10% fetal bovine serum, 100 U/ml penicillin, and 100 μg/ml streptomycin at 37 °C in a humid atmosphere of 5% $CO_2$/95% air. As for AsPC-1 and PANC-1, upon reaching 80% confluence, the medium was removed, the cells were washed in phosphate-buffered saline (PBS) and treated with various concentrations of metastin (Takeda Chemical Industries, Tsukuba, Japan) with 10% fetal bovine serum, and protein was isolated 15 min later as described below.

*Patients and tumor samples.* Pancreatic cancer tissues obtained from 30 patients who underwent pancreatectomy at our Department between January 1998 and June 2001 were used. Patients with other pancreatic malignancies, such as intraductal papillary mucinous adenocarcinoma, acinar cell carcinoma, and endocrine tumor, were excluded. Informed consent was obtained from each patient according to the institutional guidelines. Samples for mRNA expression were immediately frozen in liquid nitrogen at the time of surgery and stored at −80 °C.

*Peptide synthesis.* Fifty-four amino acid peptide, metastin, was kindly provided from Dr. T. Ohtaki, Takeda Chemical Industries [5]. We synthesized 3 short peptide variants of metastin, which were defined as FM053a2TFA, FM059a2TFA, and FM052a4TFA. The sequences of these peptides are as follows:

FM053a2TFA: Gu-Amb-Phe-Gly-Leu-Arg-Trp-$NH_2$,
FM059a2TFA: Ac-Trp-Asn-Arg-Phe-Gly-Leu-Arg-Trp-$NH_2$,
FM052a4TFA: Bis(Py)-Amb-Phe-Gly-Leu-Arg-Trp-$NH_2$.

These peptides were selected by screening from various truncated forms of KiSS1 peptide and modified peptides for gaining almost the same internal signals with metastin through the receptor using reporter gene assay in yeast.

All reagents for peptide synthesis were purchased from Watanabe Chemical Industries (Hiroshima, Japan), NovaBiochem (Darmstadt, Germany), Nacalai Tesque (Kyoto, Japan), and Wako Pure Chemical Industries (Osaka, Japan). Ion-spray mass spectra were obtained with a Sciex APIIIIE triple quadrupole mass spectrometer. Protected peptide-resins were manually constructed on Fmoc-NH-SAL resin by Fmoc-based solid-phase peptide synthesis. Trt for Asn and Pbf for Arg were employed for side-chain protection. In the synthesis of FM052a and FM053a, amino-group modifications were performed after coupling of 4-(aminomethyl)benzoic acid, respectively. Reductive amination using pyridine-2-aldehyde and $NaBH_3$ (OAc) provided the protected resin for FM052a. Treatment with 1H-pyrazole-1-carboxamidine hydrochloride and *N*,*N*-diisopropylethylamine gave the resin for FM053a. Deprotection/cleavage by treatment of the peptide resins with a mixture of TFA-thioanisole-*m*-cresol-$H_2O$-1,2-ethanedithiol-triisopropylsilane (80:5:5:5:2.5:2.5, v/v) followed by purification by reverse phase HPLC (Cosmosil 5C18-ARII column, Nacalai Tesque, Japan, 20 × 250 mm) yielded the peptides. FM059a was prepared by N-terminal acetylation of the protected octapeptide, subsequent deprotection/cleavage, and HPLC purification as well.

*Quantitative RT-PCR.* To monitor gene expression, we used quantitative real-time RT-PCR analysis [13–15]. Briefly, within the amplicon defined by a gene-specific PCR primer pair, an oligonucleotide probe labeled with 2 fluorescent dyes is created and designated as TaqMan probe. As long as the probe is intact, the emission of the reporter dye (6-carboxy-fluorescein, FAM) at the 5′-end is quenched by the second fluorescence dye (6-carboxy-tetramethyl-rhodamine, TAMRA) at the 3′-end. During the extension phase of PCR, the polymerase cleaves the TaqMan probe, resulting in a release of the reporter dye. The increasing amount of reporter dye emission is detected by an automated sequence detector combined with analysis software (ABI Prism 7700 Sequence Detection System; PE Applied Biosystems). The conditions of the reaction were according to the manufacturer's protocol. Five microliters of cDNA (reverse transcription mixture) with 25 μl TaqMan Universal PCR Master Mix (PE Applied Biosystems) and oligonucleotides at a final concentration of 0.3 μM for primers and 0.2 μM for the TaqMan hybridization probe were analyzed in a 50-μl volume.

The following primers and TaqMan probes were used for analysis. The KiSS1 specific primers were

5′-ACTCACTGGTTTCTTGGCAGC-3′ (upstream primer),
5′-ACCTTTTCTAATGGCTCCCCA-3′ (downstream primer), and
5′ (FAM)-ACTGCTTTCCTCTGTGCCACCCACT-(TAMRA)3′ (TaqMan probe).

The hOT7T175 specific primers were

5′-CGACTTCATGTGCAAGTTCGTC-3′ (upstream primer),
5′-CACACTCATGGCGGTCAGAG-3′ (downstream primer), and
5′ (FAM)-ACTACATCCAGCAGGTCTCGGTGCAGG-(TAMRA)3′ (TaqMan probe).

The thermal cycle parameters were 95 °C for 10 min (for heat activation of *Taq*-Polymerase), followed by 40 cycles of 95 °C for 15 s and 60 °C for 1 min. Assessment of GAPDH RNA for quality and normalization was done with the TaqMan GAPDH Control Reagent Kit (PE Applied Biosystems) which utilizes standard TaqMan probe chemistry.

*Protein extraction and Western blotting.* Cells were collected into microtubes with a cell scraper and lysed for 60 min in phosphorylation-inhibitory RIPA buffer containing 50 mM Hepes (pH 7.0), 250 mM NaCl, 0.1% Nonidet P-40, 1 mM phenylmethylsulfonyl fluoride (PMSF), and 20 μg/ml gabexate mesilate, and then the lysate was sonicated for 10 s. Total extracts were cleaned by centrifugation at 12,000 rpm for 10 min at 4 °C and the supernatants were collected. Protein concentrations were measured using a protein assay kit (Tonein-TP, Otsuka Pharmaceutical, Tokyo, Japan). The lysates were resuspended in one volume of the gel loading buffer which contained 50 mM Tris–HCl (pH 6.7), 4% SDS, 0.02% bromophenol blue, 20% glycerol and 4% 2-mercaptoethanol, and then boiled at 95 °C for 90 s. The extracted protein was subjected to Western blotting, as previously described [16]. In brief, 30-μg aliquots of protein were size-fractionated to a single dimension by SDS–PAGE (12% gels) and transblotted to a 0.45-μm polyvinylidene difluoride membrane (Bio-Rad, Richmond, CA) in a semidry electroblot apparatus (Bio-Rad, Richmond, CA). The blots were then washed 3 times with TBST buffer and incubated for 2 h at RT in the first antibody solution containing anti-phospho-ERK antibody (pTEpY, Promega, Madison, WI), anti-phosphop38 MAPK (pTGpY, Promega, Madison, WI) or anti-phosphoJNK (pTPpY, Promega, Madison, WI), 0.2% I-block (Promega, Madison, WI). After 3 washings in TBST buffer, the blots were incubated for 1 h at RT with horseradish peroxidase-conjugated anti-rabbit IgG at a 1:2000 dilution with TBST buffer. After 3 washings in TBST buffer, membranes were treated with enhanced chemiluminescence reagents (Amersham Life Sciences, Amersham, UK) according to the manufacturer's protocol. Membranes were exposed to X-ray film for 50–60 s. Protein expression was measured by ATTO densito-analyzer system AE-6920M (ATTO Corporation, Tokyo Japan) and the quantity was expressed numerically. The quantity of the target protein was divided by that of β-actin and relative intensities were calculated.

*Cell proliferation assay.* AsPC-1 and PANC-1 cells ($1 \times 10^4$ cells/3 cm diameter dish) were seeded in 10% FBS medium and incubated with increasing doses of metastin for 48 and 96 h. Cells were trypsinized and cell numbers were counted using hematocytometer.

*Cell migration assay and Matrigel invasion assays.* A polyvinylpyrrolidone-free polycarbonate framed filter (8 μm pores) was set in a chamber (Corning Coster, Cambridge, MA). Cells ($2 \times 10^6$ cells in 200 μl RPMI1640 for AsPC-1 and in 200 μl DMEM for PANC-1) and designated concentrations of peptide were added to the upper chamber and incubated at 37 °C for 12 h to allow migration to the lower chamber, which contained 10% FBS/RPMI1640 for AsPC-1 or 5% FBS/DMEM for PANC-1 as a chemoattractant. After removing non-migrating cells with a cotton swab from the upper surface of the membrane, cells on the lower surface were fixed, stained with Diff-Quick (International Reagent, Kobe, Japan). For quantification, cells were counted under a microscope in 5 predetermined fields at 200×.

Cells and peptide ($2 \times 10^6$ cells in 200 μl RPMI1640 for AsPC-1 and in 200 μl DMEM for PANC-1) were added to a Matrigel-coated Transwell (8 μm pores, Becton–Dickinson Labware, Bedford, MA) and incubated at 37 °C for 12 h versus a lower chamber containing 10% FBS/RPMI1640 for AsPC-1 or 5% FBS/DMEM for PANC-1. After removing the Matrigel and cells from the upper surface of the membrane, cells on the lower surface were fixed, stained with Diff-Quick and the number quantified as well. Invasion index was defined as the number of invaded cells per that of migrated cells.

*Statistical analyses.* The comparative statistical evaluations among groups in the densitometry or in the migratory activity were first performed by a two-way analysis of variance for repeated measures, followed by a post hoc Tukey test. To compare the mRNA levels in pancreatic tissues, Wilcoxon's rank sum test was performed. All assays were performed 3 times independently. Statistical analyses were done using JMP statistical software (version 3.02). Probability value of $<0.05$ was considered significant.

## Results

### *Expression of KiSS1 and hOT7T175 in pancreatic cancer tissues*

First, we measured the mRNA expression levels of KiSS1 and hOT7T175 in 30 pancreatic cancer tissues and in 5 adjacent normal pancreatic tissues. All the normal pancreatic tissues (5/5) and 14/30 of pancreatic ductal carcinoma tissues expressed KiSS1 mRNA (Fig. 1A). The expression level of KiSS1 mRNA in

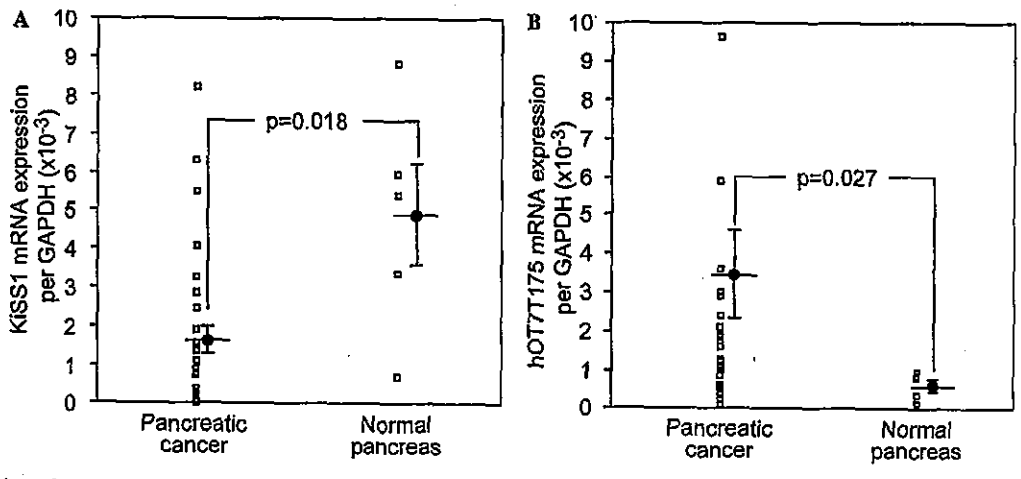


Fig. 1. Expression of KiSS1 mRNA and hOT7T175 mRNA in pancreatic cancer tissues. The KiSS1 mRNA and hOT7T175 mRNA in pancreatic cancer ($n = 30$) and normal pancreatic tissues ($n = 5$) were measured by real-time RT-PCR. The level of KiSS1 mRNA in pancreatic cancer tissues was significantly lower than that of normal pancreatic tissues ($p = 0.018$). The level of hOT7T175 mRNA in pancreatic cancer tissues was significantly higher than that of normal pancreatic tissues ($p = 0.027$).

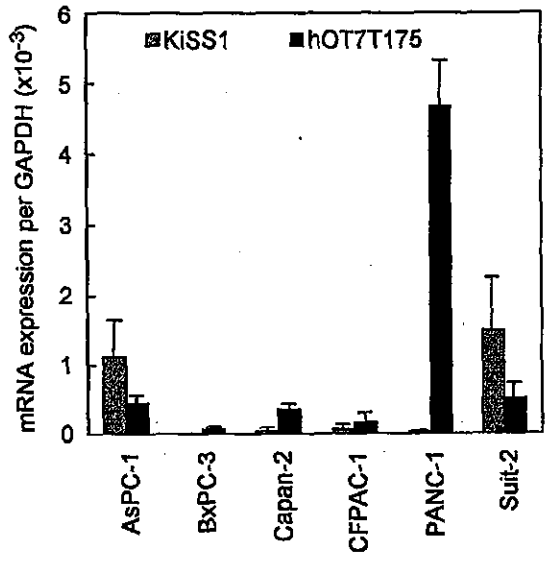


Fig. 2. Expression of KiSS1 mRNA and hOT7T175 mRNA in pancreatic cancer cell lines. The KiSS1 mRNA and hOT7T175 mRNA in pancreatic cancer cells were measured by real-time RT-PCR. AsPC-1 and SUIT-2 showed high level of metastin mRNA expression and other 4 cell lines showed very low level of expression. In contrast, all cell lines expressed hOT7T175 mRNA. PANC-1 cell most highly expressed hOT7T175 mRNA. Measurements were repeated three times and data are expressed as means ± SEM.

pancreatic cancer tissues was significantly lower than normal pancreatic tissues ($p = 0.018$). In contrast, all the pancreatic cancer tissues (30/30) and normal pancreatic tissues (5/5) expressed KiSS1 receptor hOT7T175 mRNA, and the expression level of hOT7T175 mRNA in pancreatic cancer tissues was significantly higher than that of normal tissues ($p = 0.027$) (Fig. 1B). We tested paired samples from 5 patients (cancer and normal tissues from each patient). The expression of hOT7T175 was higher in cancer tissue than the adjacent normal pancreatic tissue in all the 5 paired samples.

*Expression of KiSS1 and hOT7T175 in pancreatic cancer cell lines*

We next measured the expression of KiSS1 mRNA and hOT7T175 mRNA in 6 pancreatic cancer cell lines (Fig. 2). Among 6 pancreatic cancer cell lines, AsPC-1 and SUIT-2 showed high level of KiSS1 mRNA expression and the other 4 cell lines showed a very low level of expression. In contrast, all cell lines expressed hOT7T175 mRNA at various degrees. PANC-1 cell most strongly expressed hOT7T175 mRNA. According to these results, we chose AsPC-1 cell line as a representative of high KiSS1 and low hOT7T175, and chose PANC-1 cell line as that of low KiSS1 and high hOT7T175. We used these two cell lines in the following experiments.

*Effects of exogenous metastin on proliferation, migration, and invasion through endogenous metastin receptor*

We examined the effect of exogenous metastin on pancreatic cancer cell proliferation. Metastin peptide was added to AsPC-1 and PANC-1 cells in the phase of exponential growth at final concentrations of 0, 0.1, 1, and 10 μM for 48 and 96 h. The addition of metastin had no effects on cell proliferation of AsPC-1 and PANC-1.

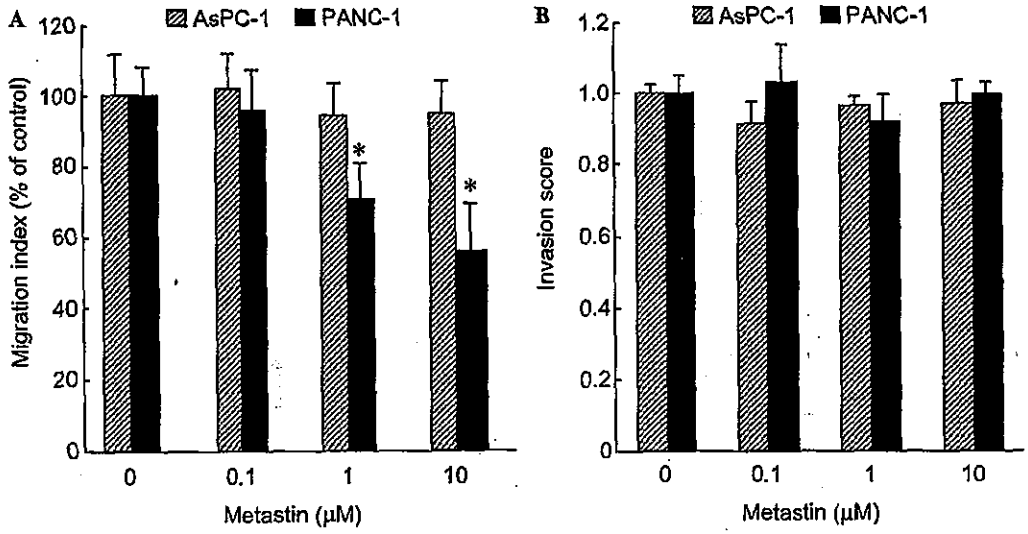


Fig. 3. Effects of exogenous metastin on migration and invasion of pancreatic cancer cells. (A) Effect of metastin on migration of pancreatic cancer cells. Cells were treated with various concentrations of metastin for 12 h. Metastin at 1 and 10 μM significantly suppressed migratory activity of PANC-1 cells. (B) Effect of metastin on invasion of pancreatic cancer cells. Cells were treated with various concentrations of metastin for 12 h. Invasion activity was not affected by tested concentrations of metastin in both AsPC-1 and PANC-1. Experiments were repeated three times and data are expressed as means ± SEM. * Represents $p < 0.05$ against control.

Next, we tested the effect of metastin on migration and invasion of these cell lines. The migration of AsPC-1 was not significantly affected by metastin, while PANC-1 was significantly inhibited by metastin at 1 and 10 μM ($p < 0.05$) (Fig. 3A). The invasion of the two cell lines was not significantly affected by metastin (Fig. 3B).

*Effects of metastin on MAPK activation in AsPC-1 and PANC-1 cells*

We analyzed the activation of MAPK by metastin. Cancer cells in exponential phase were incubated in serum containing medium and then transferred to 1% BSA medium with metastin as described in the section of migration and invasion assay. After incubation with metastin for 15 min, ERK1/2, p38, and JNK1/2 were investigated by immunoblotting (Fig. 4). Protein expression was measured by ATTO densito-analyzer system AE-6920M (ATTO Corporation, Tokyo Japan) and the relative intensity was expressed numerically (Fig. 5). Metastin induced a significant increase of pERK1 in AsPC-1 cells at 1 and10 μM and in PANC-1 at 0.1–10 μM (Fig. 5A). Metastin induced a significant increase of pp38 in PANC-1 cells at 10 μM (Fig. 5B).

*Effects of short variant forms of metastin on proliferation and migration of hOT7T175 expressing pancreatic cancer cells*

We analyzed the effects of metastin and newly synthesized short peptides, FM053a2TFA, FM059a2TFA, and FM052a4TFA, on PANC-1 cells which highly express hOT7T175. We found that the cell growth was not affected by these 3 peptides. In migration assay, metastin, FM059a2TFA, and FM052a4TFA significantly inhibited the migration of PANC-1 cells (Fig. 6). We examined the activation of ERK1/2, p38, and JNK by these variant forms and found that ERK1 and p38 were activated by metastin and all variant forms of metastin (Fig. 7).

## Discussion

In this study, we have demonstrated for the first time that hOT7T175 is expressed in pancreatic cancer tissues, but KiSS1 is less expressed when compared to normal pancreatic tissues. These results are in agreement with the analysis by other investigators in ovarian cancer, breast cancer, and colon cancer [2,5]. Several reports indicated that KiSS1 and its receptor hOT7T175 are also highly expressed in placenta [4,5]. The placenta is an invasive tissue, and there are similarities in the behavior of invading cancer cells and that of invading placenta cells [17]. It is possible that KiSS1 and hOT7T175 may constitute a common mechanism in both of these processes, whereas the correlations of clinicopathological factors such as distant metastasis and invasion with KiSS1/hOT7T175 function have not been clearly proved yet.

We next demonstrated that PANC-1 cells, which express hOT7T175, showed significant suppression of cell migration with concomitant activation of ERK1 but not

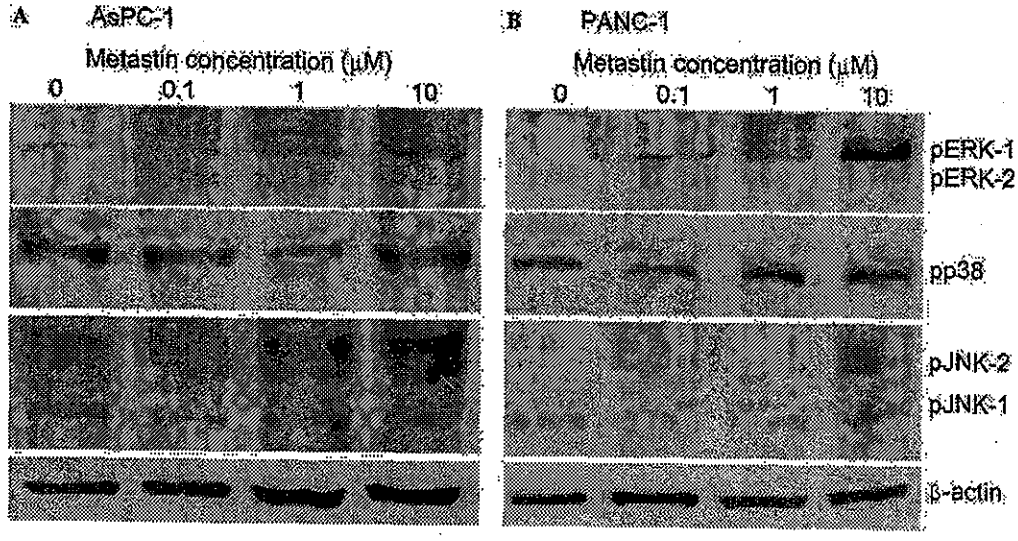


Fig. 4. Effects of metastin on MAPK activation in AsPC-1 and PANC-1 cells. AsPC-1 and PANC-1 cells were treated with various concentrations of metastin for 15 min. Western blot analysis identified double band corresponding to phosphorylated ERK1 (pERK1) and phosphorylated ERK2 (pERK2), single band of phosphorylated p38 (pp38), and double band showing phosphorylated *JNK1* (p*JNK1*) and phosphorylated *JNK2* (p*JNK2*). pERK1 was augmented in AsPC-1 by metastin at 1 and 10 μM and in PANC-1 by metastin at 0.1, 1, and 10 μM. p38 was augmented in PANC-1 by metastin at 10 μM.

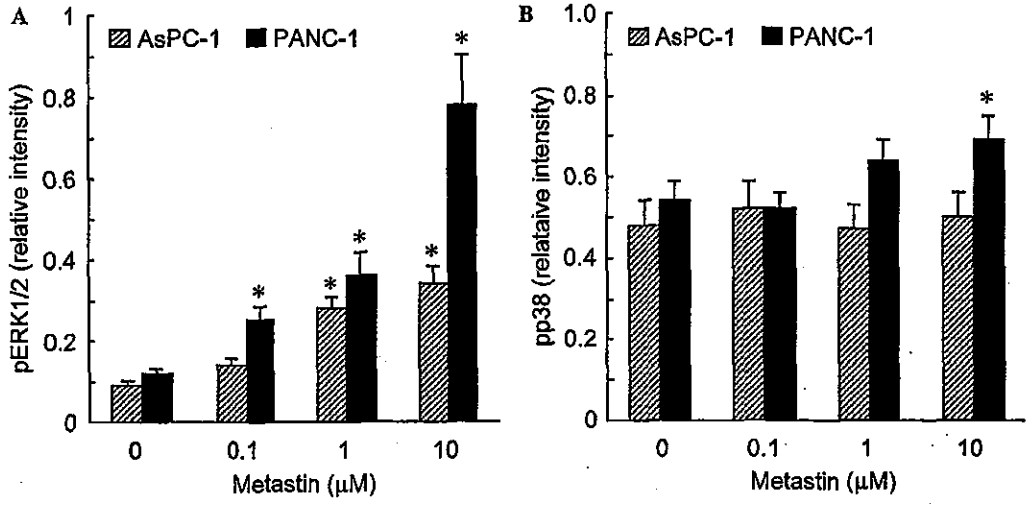


Fig. 5. Effects of metastin on pERK1/2 and of pp38 in AsPC-1 and in PANC-1 cells. AsPC-1 and PANC-1 cells were treated with various concentrations of metastin for 15 min. Protein expression of pERK1/2 or pp38 was measured by a densito-analyzer system and the quantity was expressed numerically. The quantity of the protein was divided by that of β-actin and the relative intensities were calculated. Metastin induced a significant increase of pERK1 in AsPC-1 cells at 1 and 10 μM and in PANC-1 at 0.1–10 μM (A). Metastin induced a significant increase of pp38 in PANC-1 cells at 10 μM (B). Experiments were repeated three times and data are expressed as means ± SEM. * Represents $p < 0.05$ against control.

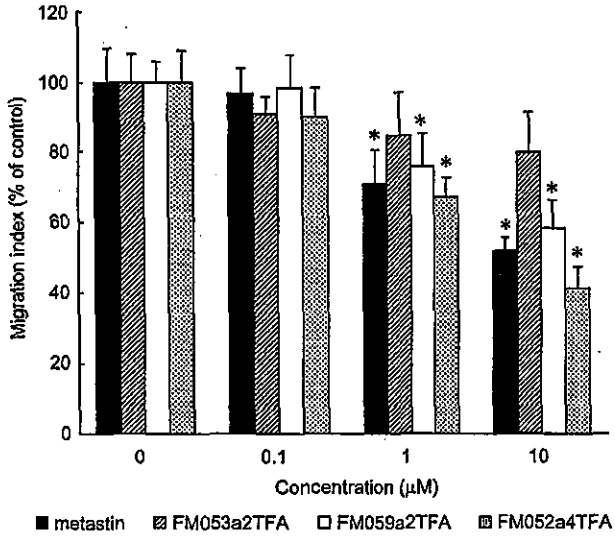


Fig. 6. Effects of short variant forms of metastin on migration of hOT7T175 expressing pancreatic cancer cells. The effect of newly synthesized short variant forms of metastin on migration of PANC-1 cells was evaluated. Metastin, FM059a2TFA, and FM052a4TFA significantly inhibited the migration activity of PANC-1 cells. Experiments were repeated three times and data are expressed as means ± SEM. * Represents $p < 0.05$ against control.

of JNK1/2 in response to exogenous metastin, while AsPC-1 cells with low expression of hOT7T175 revealed comparatively less response. Of note, the cell growth suppression was not observed both in PANC-1 and in AsPC-1, that is consistent with the previous results in melanoma and in breast cancer cells [1,2]. In contrast, in other types of cells, KiSS1 product was reported to activate ERKs and to inhibit cell proliferation [7]. These controversial results suggest that the proliferative characteristics were not a property shared by this receptor. Rather this, ERK activation may be involved in suppression of the tumor cell motility. In our study, suppression of the motility of PANC-1 cells was concomitant with the activation of ERK pathway. Moreover, as demonstrated by the newly synthesized short peptide treatment, the rate of ERK activation is in proportion to the suppression of migration.

Activation of MAP kinase and p38 has been described in hOT7T175 transfected Chinese hamster ovary cells (CHO cells) [7]. However, it has been shown that only MAP kinase but not p38 was activated with metastin treatment in anaplastic thyroid cancer cells ARO, which endogenously express hOT7T175 [18]. This discrepancy may be partly accounted by the expression level of hOT7T175 and may be by the cell specificity. In our experiment, PANC-1 cells with high expression of hOT7T175 showed activation of ERK1 and p38, while AsPC-1 cells with less hOT7T175 expression did not. These results may indicate the necessity of strong metastin-hOT7T175 signals on p38 activation in cancer cells.

We found metastin did not suppress invasion of PANC-1 and AsPC-1 cells, although several authors have reported that metastin suppresses invasion of melanoma and breast cancer cells [2,5]. The inhibitory effect on invasion could be explained by the report that showed that KiSS1 represses the invasion of HT1080 cells through decreased type 4 collagenase (MMP-9) expression and downregulation of NF-κB [3]. In pancreatic cancer tissues, we previously reported that active

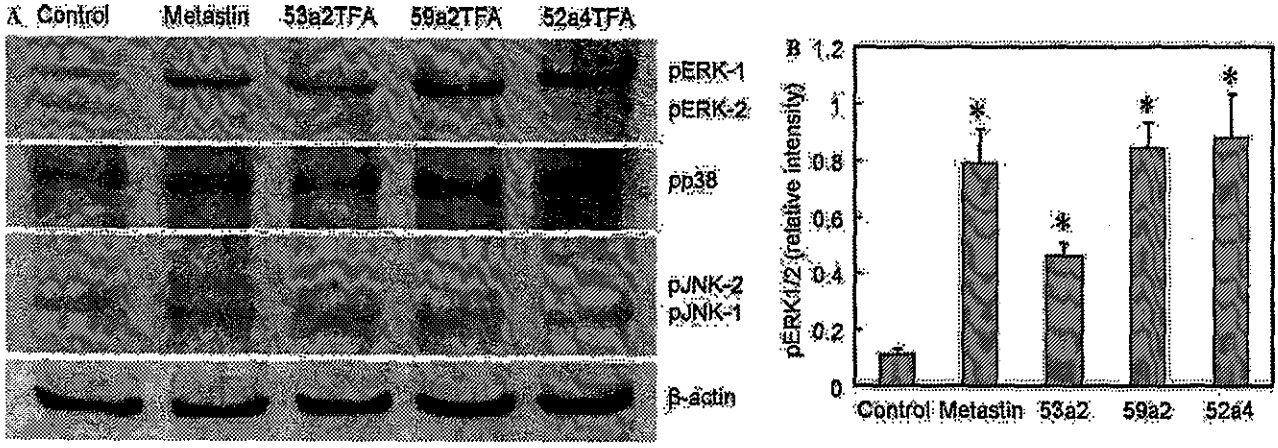


Fig. 7. Effects of short variant forms of metastin on MAPK activation in hOT7T175 expressing pancreatic cancer cells. (A) The activation of ERK1/2, p38, and JNK ERK1 activation by metastin and short variant forms of metastin was observed in PANC-1 cells. (B) pERK1 expression was measured by a densito-analyzer system, the quantity of the protein was divided by that of β-actin, and the relative intensities were calculated. In PANC-1 cells, ERK1 was significantly activated by metastin and all variant forms of metastin. Experiments were repeated three times and data are expressed as means ± SEM. * Represents $p < 0.01$ againstcontrol.

form of MMP-2 was detected in all samples; however, active form of MMP-9 was seen in only 21% of the samples [19]. Because latent forms of MMP-2 and MMP-9 were expressed in all pancreatic cancer tissues, MMP-9 may not mainly contribute to cancer invasion when compared to MMP-2. This might be one of the reasons why metastin did not affect invasion of PANC-1 and AsPC-1 cells. To our knowledge, there has been no other investigation on migration or invasion of cancer cells which endogenously express hOT7T175.

Our newly synthesized short variant forms of metastin showed significant suppression on motility of PANC-1 cells. These peptides are composed of 6–9 amino acids, suggesting that at most 10 amino acids of the C-terminus of metastin-54 will be sufficient for its binding affinity and function. However, FM053a2TFA is less effective in suppressing migration of PANC-1 cells when compared to other two compounds or metastin-54. Interestingly, the suppressive activity was in proportion to the ERK activation rates. Much remains to be understood about how effective they will block migration and how the peptides could be stably delivered to the tumors. The effective short peptide has an advantage that it would not cause immune responses if it could be given to patients orally.

In conclusion, we demonstrated that pancreatic cancer tissues express hOT7T175 and low expression of KiSS1 when compared to normal pancreatic tissues. The exogenous metastin and the variant forms of metastin suppress migration of hOT7T175-expressing pancreatic cancer cells and activate ERK1 and p38. Our results suggest that hOT7T175 may be one of the promising targets against cancer cell functions that are relevant to metastasis, and that short variant forms of metastin could be an anti-metastatic agent to pancreatic cancer.

## Acknowledgment

This study was supported by a Grant-in-Aid for Scientific Research (#15390395) from the Ministry of Education, Culture, Sports, Science and Technology of Japan.

## References

[1] J.H. Lee, M.E. Miele, D.J. Hicks, K.K. Phillips, J.M. Trent, B.E. Weissman, D.R. Welch, J. Natl. Cancer Inst. 88 (1996) 1731–1737.
[2] J.H. Lee, D.R. Welch, Cancer Res. 57 (1997) 2384–2387.
[3] C. Yan, H. Wang, D.D. Boyd, J. Biol. Chem. 276 (2001) 1164–1172.
[4] A.I. Muir, L. Chamberlain, N.A. Elshourbagy, D. Michalovich, D.J. Moore, A. Calamari, P.G. Szekeres, H.M. Sarau, J.K. Chambers, P. Murdock, K. Steplewski, U. Shabon, J.E. Miller, S.E. Middleton, J.G. Darker, C.G. Larminie, S. Wilson, D.J. Bergsma, P. Emson, R. Faull, K.L. Philpott, D.C. Harrison, J. Biol. Chem. 276 (2001) 28969–28975.
[5] T. Ohtaki, Y. Shintani, S. Honda, H. Matsumoto, A. Hori, K. Kanehashi, Y. Terao, S. Kumano, Y. Takatsu, Y. Masuda, Y. Ishibashi, T. Watanabe, M. Asada, T. Yamada, M. Suenaga, C. Kitada, S. Usuki, T. Kurokawa, H. Onda, O. Nishimura, M. Fujino, Nature 411 (2001) 613–617.
[6] A. Hori, S. Honda, M. Asada, T. Ohtaki, K. Oda, T. Watanabe, Y. Shintani, T. Yamada, M. Suenaga, C. Kitada, H. Onda, T. Kurokawa, O. Nishimura, M. Fujino, Biochem. Biophys. Res. Commun. 286 (2001) 958–963.
[7] M. Kotani, M. Detheux, A. Vandenbogaerde, D. Communi, J.M. Vanderwinden, E. Le Poul, S. Brezillon, R. Tyldesley, N. Suarez-Huerta, F. Vandeput, C. Blanpain, S.N. Schiffmann, G. Vassart, M. Parmentier, J. Biol. Chem. 276 (2001) 34631–34636.
[8] D.K. Lee, T. Nguyen, G.P. O'Neill, R. Cheng, Y. Liu, A.D. Howard, N. Coulombe, C.P. Tan, A.T. Tang-Nguyen, S.R. George, B.F. O'Dowd, FEBS Lett. 446 (1999) 103–107.
[9] A. West, P.J. Vojta, D.R. Welch, B.E. Weissman, Genomics 54 (1998) 145–148.
[10] G. Rigaud, P.S. Moore, G. Zamboni, S. Orlandini, D. Taruscio, S. Paradisi, N.R. Lemoine, G. Kloppel, A. Scarpa, Int. J. Cancer 88 (2000) 772–777.

[11] T. Yatsuoka, M. Sunamura, T. Furukawa, S. Fukushige, T. Yokoyama, H. Inoue, K. Shibuya, K. Takeda, S. Matsuno, A. Horii, Am. J. Gastroenterol. 95 (2000) 2080–2085.
[12] T. Harada, K. Okita, K. Shiraishi, N. Kusano, T. Furuya, A. Oga, S. Kawauchi, S. Kondoh, K. Sasaki, Oncology 62 (2002) 251–258.
[13] I. Bieche, I. Laurendeau, S. Tozlu, M. Olivi, D. Vidaud, R. Lidereau, M. Vidaud, Cancer Res. 59 (1999) 2759–2765.
[14] T.D. Schmittgen, B.A. Zakrajsek, A.G. Mills, V. Gorn, M.J. Singer, M.W. Reed, Anal. Biochem. 285 (2000) 194–204.
[15] A. Yuan, C.J. Yu, K.T. Luh, W.J. Chen, F.Y. Lin, S.H. Kuo, P.C. Yang, Lab. Invest. 80 (2000) 1671–1680.
[16] M. Wada, R. Doi, R. Hosotani, J.U. Lee, K. Fujimoto, T. Koshiba, Y. Miyamoto, S. Fukuoka, M. Imamura, Pancreas 15 (1997) 176–182.
[17] M.J. Murray, B.A. Lessey, Semin. Reprod. Endocrinol. 17 (1999) 275–290.
[18] M.D. Ringel, E. Hardy, V.J. Bernet, H.B. Burch, F. Schuppert, K.D. Burman, M. Saji, J. Clin. Endocrinol. Metab. 87 (2002) 2399.
[19] T. Koshiba, R. Hosotani, M. Wada, Y. Miyamoto, K. Fujimoto, J.U. Lee, R. Doi, S. Arii, M. Imamura, Cancer 82 (1998) 642–650.

# Expression of pancreatic duodenal hoemobox-1 in pancreatic islet neogenesis after surgical wrapping in rats

**Ryo Hosotani, MD, Jun Ida, MD, Masafumi Kogire, MD, Koji Fujimoto, MD, Ryuichiro Doi, MD,** *and* **Masayuki Imamura, MD,** *Kyoto, Japan*

***Background.*** *Surgical wrapping (SW) of the pancreas causes islet neogenesis in rodents. Pancreatic duodenal hoemobox-1 (PDX-1) is one of the transcriptional factors needed by pancreatic stem cells to develop a mature pancreas. The purpose of this study was to determine whether islet neogenesis arises from ductal cells and whether PDX-1 is involved in this process.*

***Methods.*** *SW consisted of nonocclusive wrapping of the pancreas in rats. The wrapped pancreas was then harvested, insulin content was measured, and immunohistochemical analysis for insulin, cytokeratin, and PDX-1 was performed.*

***Results.*** *The endocrine area of the wrapped pancreas significantly increased after SW. Double immunostaining identified cells positive for both insulin and cytokeratin in or along the epithelial cell lining of the ductal structures and in the centroacinar cells. PDX-1–positive cells were detected in both control islets and islets examined after SW, but these cells were observed in the exocrine area only after SW. Double staining also showed that cells positive for PDX-1 but negative for insulin were present in the exocrine area 1 day after SW and that cells positive for both PDX-1 and insulin had developed 3 days after SW.*

***Conclusions.*** *In the process of adult islet neogenesis after SW, cells in the acini and ductal structures developed into PDX-1–expressing cells, supposedly progenitor cells, which in turn became insulin-producing cells and thus might be the origin of small islets. (Surgery 2004;135:297-306.)*

*From the Department of Surgery and Surgical Basic Science, Graduate School of Medicine, Kyoto University, Kyoto, Japan*

THE PANCREAS CONSISTS OF 3 TYPES of differentiated tissue: the hormone-secreting cells in the islets, the exocrine acini, and the duct tree of centroacinar cells, ductules, and ducts. During embryogenesis in rodents, presumptive islet precursor cells are first observed about halfway through the gestational period; these cells actively proliferate, differentiate, and then aggregate into mature islets.[1] New islet formation continues for approximately the first 3 weeks of life, during which a mature morphology is acquired and glucose sensing is activated. Thereafter, and throughout the lifetime of the animal, a constant, slow turnover of islets occurs.[2]

Of special interest is the regeneration of new islet cells, including insulin-producing cells, after pancreatic tissue injury as the result of a process called adult islet neogenesis. The animal models of pancreatic tissue injury include chemical destruction of B cells by streptozotocin (STZ) or alloxan, partial pancreatectomy, physical injury to the pancreas by ligation of the pancreatic duct or wrapping of the pancreas, spontaneous diabetes in non-obese diabetic mouse model, or overexpression of interferon-gamma in the pancreas.[1,3] It has been a matter of debate whether the cell-renewal process depends on the simple replication of pre-existing B cells in the islets, differentiation of latent progenitor cells of the adult pancreas, or trans-differentiation of fully differentiated cells such as acinar or ductal cells. Bonner-Weir[3] also raised the possibility that the process may occur by several pathways. Most studies have provided evidence that neogenesis is the result of differentiation of cells that act as precursors in adult ductal epithelium.[1,3]

Supported in part by the Japan Ministry of Education grant A12307026.

Accepted for publication July 3, 2003.

Reprint requests: Ryo Hosotani, MD, Department of Surgery, Kobe City General Hospital, 4-6 Port Island, Cyuo-ku, Kobe 650-0046, Japan.

0039-6060/$ - see front matter



doi:10.1016/S0039-6060(03)00394-5

However, using an experimental model of diabetes, Guz et al[4] indicate the possibility that regeneration of B cells may originate in intraislet precursor cells. The authors showed in STZ-treated mice that insulin-containing cells reappeared in the islets after STZ-mediated elimination of existing B cells and that this B-cell regeneration was significantly enhanced once normoglycemia was attained after exogenous insulin administration. There is as yet no agreement, however, on the exact mechanism of adult islet neogenesis or on the origin of putative progenitor cells and their regulation.

PDX-1, the homeodomain-containing transcriptional factor of pancreatic duodenum homeobox gene-1—also known as IPF-1, IDX-1, or STF-1—plays a critical role in pancreatic stem cell biology, since PDX-1 knockout mouse studies have demonstrated that neonatal PDX-1 −/− mice are apancreatic.[5-7] Immunohistochemical studies of mouse pancreatic development also showed that PDX-1–positive cells were initially expressed by multipotential precursors and only later became restricted to the insulin-containing B cells.[8] Several animal studies of the adult pancreas have demonstrated the occurrence of ectopic expression of PDX-1 in pancreatic ductal structures or of overexpression inside the islets.[9-13]

The purpose of this study was to determine whether islet neogenesis arises from ductal cells and whether PDX-1 is involved in this process. To test this, we conducted an immunohistochemical examination of the expression of PDX-1 after non-occlusive pancreatic wrapping in a model of islet hyperplasia (nesidioblastosis). This model is distinct from other models such as those of regeneration of both the exocrine and the endocrine pancreas after pancreatectomy or of recovery of islets after STZ chemical destruction. To identify the origin and fate of PDX-1–presenting cells, we used double immunostaining with cytokeratin and insulin.

## MATERIAL AND METHODS

**Animal preparation.** Six-week-old male Wistar rats, weighing between 176 and 204 g, were kept in a screen-bottomed cage at 22°C on a 12-hour light-dark cycle with free access to water and a standard laboratory diet. Animal care and surgery were carried out at the Institute of Laboratory Animals of Kyoto University in accordance with the institute's guide for the care and use of laboratory animals.

**Experimental design.** The surgical wrapping (SW) model was initially developed in the hamster with the use of cellophane wrapping[14,15] and was followed by the non-occlusive wrapping technique with a silk tie in rats.[16] We have adopted the rat model in this study. Briefly, SW wrapping was performed through a midline laparotomy, with the rats under anesthesia with diethylether inhalation, and the splenic lobe of the pancreas was gently freed from the transverse colon with use of a radio knife. A 2-0 silk tie was brought around the pancreas at the level of the portal vein in a gentle and non-occlusive manner, taking care not to involve other organs or splenic vessels in the tie. The abdomen was then closed; the whole procedure took approximately 10 minutes.

Pancreatic tissues were examined in 5 rats at time points of 1, 3, 7, and 14 days after surgery. Sham-operated rats served as the control. The surgically wrapped animals were anesthetized with diethylether, and the splenic lobe of the pancreas distal from the tie was removed and weighed. The proximal parts of the splenic lobes of the pancreas were frozen immediately with liquid nitrogen and stored at −80°C until further processing. The distal parts of the splenic lobes were rinsed with phosphate-buffered saline (PBS) and were immersion-fixed overnight at 4°C in 4% paraformaldehyde buffered with 0.1 mol/L sodium phosphate (pH 7.4).

**Protein extraction and insulin measurement.** All the tissue samples for the protein assay were stored at −80°C. The subsequent procedures were done at −4°C. Frozen tissues were crushed with a hammer, and small pieces of tissue were immediately suspended on ice with 5 volumes of 70% ethanol containing 0.15 mol/L HCl. The extracted tissues were homogenized with a microtip sonic homogenizer (Handy Sonic; Tomyseiko, Tokyo, Japan) for 10 seconds and incubated for more than 24 hours at −20°C. After the extracts were cleaned by centrifugation at 12,000 rpm (400g) for 10 minutes at 4°C, the supernatants were collected. Protein concentrations were measured with a protein assay kit (Tonein-TP; Otsuka Pharmaceutical, Tokyo, Japan). Insulin concentration in a tissue extract was assayed with an enzyme immunoassay kit (Glanzyme insulin-EIA TEST; Sanyo, Kyoto, Japan) according to the manufacturer's protocol. After the insulin and protein concentrations of all the samples were measured, the insulin content of the tissue was determined for each of the groups.

**Immunohistochemistry for insulin.** The following immunohistochemical procedures were performed at room temperature (RT), except for the antigen-retrieval procedure for PDX-1. The serial sections were deparaffinized in 3 changes of xylene,

rehydrated in descending concentrations of ethanol, and then washed 3 times for 5 minutes with double-distilled water (DDW). After rehydration, the sections were soaked in 3% $H_2O_2$ for 10 minutes to block endogenous peroxidase activities. After being washed with DDW 2 times for 2 minutes, the sections were incubated for 10 minutes in PBS. Insulin antibody A0564 (DAKO, Glostrup, Denmark) diluted 1/800 with PBS containing 1% bovine serum albumin (BSA) was then applied, and the sections were incubated for 30 minutes. The sections were washed 3 times with PBS for 5 minutes, a second antibody, En Vision+ (DAKO, K4003), was applied, and the sections were incubated for 30 minutes. The sections were again washed 3 times with PBS for 5 minutes, then developed for 1 to 5 minutes with diaminobenzidine-tetra-hydrochloride (DAKO, K3465) as the substrate, and washed 2 times with running water.

**Immunohistochemistry for PDX-1.** Immunohistochemical staining of PDX-1 was performed with a specific antibody for rodent PDX-1 (a generous gift from Dr C. V. Wright, Vanderbilt University, Nashville, Tenn). The specificity of the antibody is described elsewhere.[17] The immunohistochemical procedure was slightly modified in terms of the antigen-retrieval procedure for paraffin-embedded samples. After deparaffinization and rehydration, the sections were pretreated in the Target Retrieval Solution (DAKO, S3307) in a microwave (NE-TC5, Panasonic, Japan) for 20 minutes at 95°C and then cooled at RT for 20 minutes. The sections were soaked in 3% $H_2O_2$ for 10 minutes and then incubated for 10 minutes with 50 mmol/L Tris-HCl buffer containing 0.15 mol/L NaCl and 0.1% Tris-buffered saline Tween-20 (TBST). PDX-1 antibody, diluted 1/1000 with TBST containing 1% BSA, was then applied, and the sections were incubated for 60 minutes. The sections were then washed 3 times with TBST for 5 minutes, En Vision+ (DAKO, K4003) was applied, and the sections were incubated for 30 minutes. The sections were again washed 3 times with TBST for 5 minutes, developed with diaminobenzidine-tetra-hydrochloride for 1 to 5 minutes, and washed 2 times with running water.

**Double staining of insulin and cytokeratin.** The tissue sections were first treated in the manner described in the section *Immunohistochemistry for insulin* and incubated for 10 minutes in PBS. Protein K (DAKO, 3020) was then applied for 6 minutes followed by 3 washes with PBS. Cytokeratin antibody N1523 (DAKO) was applied, and the sections were incubated for 30 minutes. The sections were then washed 3 times with PBS, and cytokeratin antibody N1523 was applied at RT for 10 minutes. In the final steps, the sections were washed 3 times with PBS, developed with New Fuchsin Substrate System (DAKO, K0698) for about 2 to 3 minutes, dipped into PBS, counterstained with Mayers hematoxylin, and immediately mounted in glycergel (aqueous mounting medium).

**Double staining of PDX-1 and insulin.** The tissue sections were first treated as described in the section *Immunohistochemistry for PDX-1* and incubated for 10 minutes with TBST. The sections were then pretreated with 0.2N HCl for 20 minutes, washed 2 times with DDW for 5 minutes, and washed again 3 times with TBST for 5 minutes. Insulin antibody A0564 diluted at 1/800 with TBST containing 1% BSA was applied, and the sections were incubated for 30 minutes. The sections were then washed 3 times with TBST, and the insulin antibody was applied again at RT for 30 minutes. In the final steps, the sections were washed 3 times with TBST for 5 minutes, developed with New Fuchsin Substrate System K0698 for about 2 to 3 minutes, dipped into PBS, counterstained with Mayers hematoxylin, and mounted in glycergel.

In the double-staining technique of insulin and cytokeratin, insulin immunoreactivity (IR) was detected with 3,3'-diaminobenzidine (DAB) brown, and cytokeratin IR was detected with Fuchsin red violet. Conversely, in the double-staining technique of PDX-1 and insulin, PDX-1 IR was detected with DAB brown, and insulin IR was detected with Fuchsin red violet. Several tissue samples were exposed to nonspecific immunoglobulin G as the primary antibody to confirm specificity of the results, including the double-staining studies. No samples showed immunoreaction.

**Statistical analysis.** Pancreatic islets were identified in the samples of insulin immunohistochemistry. The endocrine area of each sample was calculated by computerized densitographic measurement (ATTO, Hamamatsu, Japan). Islet sizes were categorized as tiny ($<20\ \mu m^2$ in size), small ($20\sim50\ \mu m^2$), medium ($50\sim100\ \mu m^2$), and large ($>100\ \mu m^2$). The number of each islet category was counted in each sample. Insulin IR and PDX-1 IR were also detected in single cells outside the islet. The number of these cells was also counted in each sample. Data are expressed as the mean value ± SD. Statistical differences among each time point were assessed by analysis of variance (ANOVA). The Tukey-Kramer test for post hoc multiple comparisons was used when ANOVA was significant. All statistical analyses were done using JMP statistical software for Macintosh (Ver 3.02; SAS

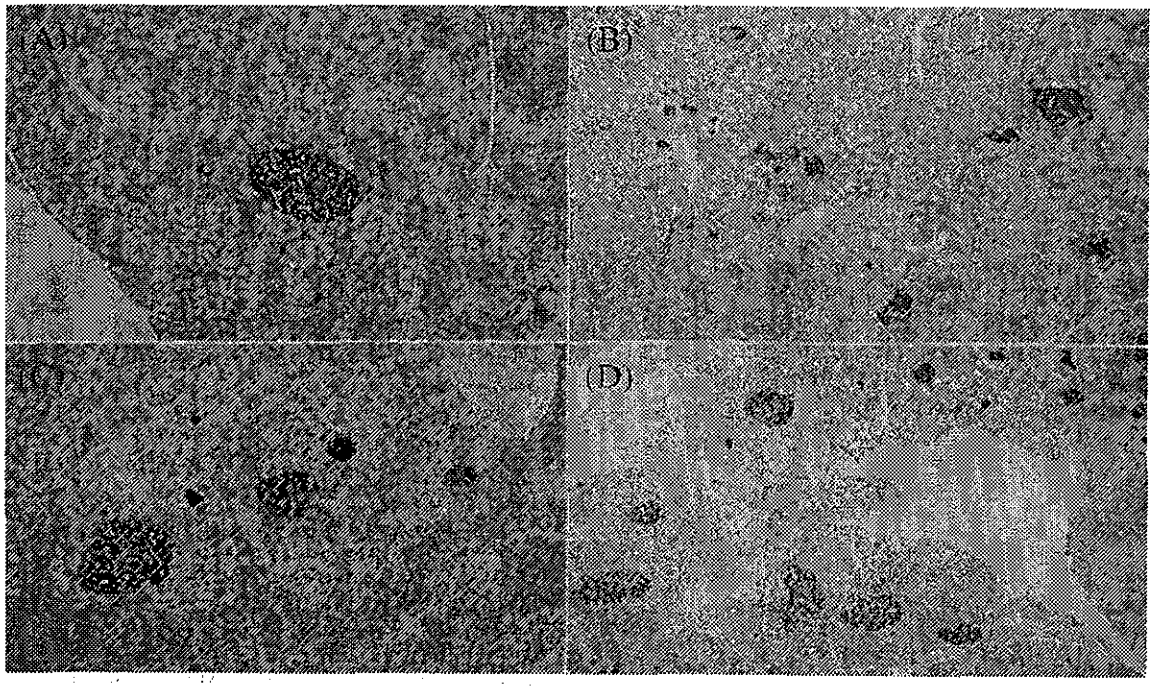


**Fig 1.** Immunohistochemical staining of insulin in the splenic lobe of the pancreas after surgical wrapping. **A,** Control; **B,** 3 days; **C,** 7 days; and **D,** 14 days after surgical wrapping. There was a marked increase in the number of islets after surgical wrapping. (Original magnification ×100.)

**Table I.** Gross changes of the splenic lobe after surgical wrapping

| | | *Days after Surgical Wrapping* | | | |
|---|---|---|---|---|---|
| | *Control* | *1* | *3* | *7* | *14* |
| Weight (mg) | 310 ± 40 | 305 ± 40 | 300 ± 10 | 310 ± 40 | 300 ± 20 |
| Insulin content (μU/mg prot) | 74 ± 16 | 60 ± 15 | 97 ± 13 | 115 ± 23 | 119 ± 25 |
| Endocrine area (%) | 1.2 ± 0.3 | 1.3 ± 0.4 | 1.5 ± 0.4 | 2.2 ± 0.5 | 2.6 ± 0.4* |

mean ± SD, n = 5.
*$P < .05$ vs control (ANOVA).

Institute, Cary, NC). The level of significance was defined as $P < .05$.

## RESULTS

**Changes in pancreatic islets after SW.** Neither edema nor atrophy of the pancreas was observed in this model. Wet weight of the splenic lobe distal from the tie was constant throughout the study period (Table I). Insulin content of the splenic lobe in control rats was 74 ± 16 μU/mg of protein. The content increased to 119 ± 25 μU/mg of protein 14 days after SW (approximately 160% of control), but these values did not reach statistical significance. Figure 1 shows a representative photograph of the immunohistochemical analysis for insulin. Three days after SW, the number of small islets increased, and weak and spotty insulin staining was seen on the circumference of the pre-existing islets. Medium and large islets showed a marked increase in number on days 7 and 14 after SW.

Calculation of the endocrine area showed that it accounted for 1.2% ± 0.3% of the total area of the pancreas in control animals and had increased significantly to 2.6% ± 0.4% 14 days after SW (Table I). To quantify the changes in islets, we calculated their number according to size (tiny, small, medium, large) for the sake of relevance (Fig 2). Tiny islets (<20 $\mu m^2$) increased during the relatively early phase, small (20~50 $\mu m^2$) and medium (50~100 $\mu m^2$) islets increased continuously, and large islets (>100 $\mu m^2$) increased in the later stages. The number of large islets had